Th-AM-Sym-1 THEORETICAL ASPECTS OF NUCLEIC ACID STRUCTURE. Wilma K. Olson, Department of Chemistry, Rutgers University, New Brunswick, New Jersey 08903.

The elaborate architecture of its monomeric repeating units makes the nucleic acid a difficult system to comprehend at the detailed structural level. Even a very crude description of local flexibility generates an untold number of three-dimensional spatial arrangements. This conformational complexity simply stems from the many ways that the variable parameters in the sugar-phosphate backbone can achieve a particular positioning of adjacent bases. By focusing on base morphology rather than on the chain backbone, one can begin to unravel the conformational complexities of the nucleotide repeating unit and also understand the effects of primary chemical sequence upon overall nucleic acid structure. The energetically preferred arrangements of specific base sequences yield distinct morphological patterns. These preferences, in turn, have pronounced effects on the macroscopic properties of long helical chains. The variations in base morphology resulting from the higher order folding of the B-DNA double helix further suggest the important influence of primary sequence upon nucleic acid properties and interactions. (Supported by USPHS grants GM-20861 and GM-34809).

Th-AM-Sym-2 NMR STUDIES OF DRUG-DNA COMPLEXES IN AQUEOUS SOLUTION: Xiaolian Gao and Dinshaw Patel. Department of Biochemistry and Molecular Biophysics, Columbia University, NY, NY 10032.

Two dimensional proton NMR studies are reported on a series of drug-DNA complexes in aqueous solution aimed at defining the stacking, hydrogen bonding and hydrophobic interactions stabilizing complex formation.

Echinomycin belongs to the quinoxaline family of antitumor agents which bisintercalate into DNA. Footprinting and X-Ray studies have established minor groove binding with the quinoxaline chromophores bisintercalating on either side of dC-dG steps. NMR studies have been undertaken on echinomycin complexes with self-complementary d(ACGT), d(TCGA), d(GCGC), d(CCGG), d(AAACGTTT) and d(ATACGTAT) duplexes in aqueous solution. The structural conclusions in solution will be compared with those available in the crystalline state and we shall demonstrate a sequence and pH dependent switch between Watson-Crick and Hoogsteen base pairs flanking the bisintercalation site.

Chromomycin, an aureolyic antitumor agent, recognizes and complexes duplex DNA at dG-dG sites in the presence of Mg. We shall report on detailed NMR studies on chromomycin complexes with self-complementary d(AAACGTTT) and d(TTTCGAAA) duplexes in Mg-containing aqueous solution. This study focuses on differentiating between minor and major groove binding and establishing contacts between the DNA and the aglycon and hexapyranoses of the antitumor agent.

Several other antitumor drug-DNA complexes are also currently being investigated by NMR techniques and these results will be presented at the Symposium.

Th-AM-Sym-3 NUCLEIC ACID BRANCHED JUNCTIONS. Nadrian C. Seeman*, Neville Kallenbach[+], Mair Churchill[#], Thomas Tullius[#], Colin Newton*, Jung-Huei Chen*, Mary Petrillo*, John Mueller*, Börries Kemper**, and Richard Cunningham*, *SUNY/Albany, NY 12222, [+]New York University, NY, NY 10003, [#]Johns Hopkins University, Baltimore MD 21218 and **University of Köln, West Germany.

Nucleic acid junctions are stable analogs of ephemeral branched structures, such as Holliday intermediates, which arise in the course of recombination. We construct these complexes from individual oligonucleotide strands whose symmetry-minimized sequence directs their unique association. The bulk of our work has been done with a 4-arm junction composed of 4 hexadecanucleotides and its derivatives, but in addition we have constructed junctions containing 3, 5 and 6 arms. Both 3-arm and 4-arm junctions have been shown by ligation experiments to be flexible over long time periods. By hydroxyl radical cleavage experiments we have determined that this junction has a strong bias in solution for a two-fold symmetric structure, with only two of the four strands strongly protected near the branch site. The structure appears to have two unperturbed helical strands and two crossover strands, much like the Sigal-Alberts proposal. We have shown that altering the bases which flank the branch site can reverse the crossover bias. In addition, in two cases examined, we find that the crossover bias is greater than branch point migratory biases. The hexadecamer junction is too small to be cleaved by Endonuclease VII, but the addition of one or more long arms makes it a good substrate. We have shown that the direction of cleavage by Endonuclease VII is a function of the arm to which the enzyme attaches itself, before diffusion to the branch site.

This work has been supported by grants GM-29554, ES-00117, CA-24101 and CA-37444 from the NIH.

Th-AM-Sym-4 VISUALIZATION OF THE BENDING OF DNA BY NATURAL SEQUENCE ARRANGEMENTS AND PROTEINS THAT BIND THESE SEQUENCES. Jack D. Griffith, Hsilin Cheng, Caroline Laundon, and Richard Rubin, Lineberger Cancer Research Center, University of North Carolina, Chapel Hill, North Carolina 27514. The axis of the DNA helix can be bent by proteins, DNA damaging agents, drugs, and by naturally occurring sequences. Gel electrophoresis provides a powerful tool but appears to require that the bends be planar for the DNA fragment to show a significant retardation of mobility. Using electron microscopy (EM) it has been possible to directly visualize the bending of a 200 bp highly bent DNA segment isolated from the kinetoplast DNA of Crithidia fasciculata. When this highly bent helix segment was cloned into 2 sites in pBR325 and the resulting DNA reconstituted with a limiting amount of histone proteins, the bent helix segments showed a 3 to 10 fold higher affinity for nucleosome formation. In addition, the bent helix segments were found to reside at the ends of the interwound supertwisted DNA rods as seen by EM. A highly bent helix segment was identified at the terminus of SV40 DNA replication. This segment binds histones tightly and locates at the ends of supertwisted DNA rods, but shows a relatively small retardation on gel electrophoresis, presumably due to the non-planar nature of the bend.

Th-AM-MinI-1 ENZYME DYNAMICS UNDER FLUCTUATING OR OSCILLATING CONDITIONS.

R. Dean Astumian, Bldg. 3, Room 202, Lab. of Biochemistry, NHLBI, NIH, Bethesda, MD 20892

Fundamental considerations for understanding the effects of oscillating or randomly fluctuating perturbations on an enzyme system are presented. It is shown that even for the simplest possible enzyme, demonstrating Michaelis-Menten kinetics under constant conditions, complex behavior in a nonstationary environment may be anticipated. This includes the transduction of energy from the source of the externally driven fluctuations to do chemical or transport work by "catalyzing" the reaction for which it is specific away from equilibrium. Additionally, the manifestation of experimentally observed frequency and amplitude "windows", outside of which no or reduced effects are seen, are readily understood in the context of the theoretical analysis presented. The basic relationship between enforced (internally or externally) oscillation and energy driven fluctuations or noise is discussed, with emphasis on the differences between macroscopic and microscopic pictures.

Th-AM-MinI-2 EFFICIENCY AND DISSIPATION IN NON-LINEAR CHEMICAL AND BIOLOGICAL PROCESSES.

John Ross, Department of Chemistry, Stanford University, Stanford, California 94305

The efficiency of nonlinear reaction systems, with oscillations of chemical intermediates or stable foci, can be affected by external periodic perturbations. We discuss first the efficiency of a proton pump, powered by ATP, and compare the efficiency at constant ATP concentration with that of a variable ATP concentration with given amplitude and frequency. At critical frequencies of perturbation, the efficiency can be increased by about 10%. We analyze the second example of the efficiency of a pump which maintains a given concentration gradient of FDP, ATP, F6P, and phosphate. The possibility of oscillations in chemical reactions leads to the design of chemical analogs of AC circuits which have advantages over DC chemistry.

Th-AM-MinI-3 NONLINEAR DYNAMICS IN BIOCHEMICAL AND BIOLOGICAL PROCESSES.

Benno Hess, Max-Planck-Institut fur Ernahrungsphysiologie, Dortmund, FRG

Over the last decades the extension of thermodynamics to open and far from equilibrium conditions and the development of tools for the study of nonlinear dynamics has uncovered macroscopic mechanisms of self-organization in time and space and opened experimental pathways into the complexity of dynamic structures. Indeed, the new concepts and methodologies in mathematics, physics and biology readily crossed the barriers between the classically reduced description of bounded homogeneous systems and the non-intuitive and inexhaustible richness of spatial-temporal structures in nature. Today, understanding of dynamic pattern formation is of great interest in many areas of science. This presentation deals with results of theoretical and experimental studies of typical temporal structures in chemical, enzymic and membrane-bound processes such as observed under constant or periodic substrate load and noise perturbation. We observe periodic, quasi-periodic, chaotic responses reflecting complex dynamic domains including coexistence of several attractors, hysteresis, and noise amplification. These results are complemented by investigations using 2D photometric techniques on spatial organizations of chemical and biological systems illustrating principles of signal wave propagation in macroscopic pattern formation.

Th-AM-MinI-4 NOISE-INDUCED TRANSITIONS IN BIOLOGICAL SYSTEMS W. Horsthemke, Dept. of Physics, The University of Texas, Austin, TX 78712 (Intr. by R. D. Astumian)

External random fluctuations ("noise") can impose structure on nonlinear systems that is not present when the fluctuations are absent. An example of noise-induced bistability in a biological system is presented. External noise is also a convenient probe to elucidate the dynamics of nonlinear systems.

Th-AM-MinI-5 COUPLING.

Hans V. Westerhoff, Frits Kamp and R. Dean Astumian
Lab. Mol. Biol., NIDDK and Lab. Biochem. NHLBI, NIH, Bethesda, MD 20892, USA.

Coupled reactions such as catalyzed by ion pumps are often described as an enzyme moving through a single catalytic cycle and hence necessarily carrying out both reactions [1]. Incomplete coupling of the two reactions catalyzed by the enzyme is then seen as slippage, such that it skips part of the overall cycle. A 'slip' transition is added to the catalytic cycle, such that the input reaction can proceed without driving the output reaction and the output reaction may slip in reverse without reverting the input reaction. Incomplete coupling is essentially pictured as a, perhaps minor, deviation from the perfectly coupled state.

To understand how coupling comes about in the first place, it may be instructive to start from the separate input (e.g., ATPase) and output (e.g., proton translocation across a membrane) reaction, each catalyzed by a separate subunit of an enzyme complex. In this presentation we shall discuss how nonstationary (e.g., electrical noise-like) interactions between the two subunits may lead to coupling of their reactions.

(Supported in part by the Netherlands Organization for the advancement of pure research (ZWO).)

1. Westerhoff H.V. and Van Dam K. (1987) Thermodynamics and Control of Biological Free-Energy Transduction, Elsevier, Amsterdam.

Th-AM-MinI-6 TRANSDUCTION OF ENERGY FROM OSCILLATING ELECTRIC FIELDS BY MEMBRANE ATPases THROUGH ELECTROCONFORMATIONAL COUPLING. Tian Yow Tsong[1], Daosheng Liu[1], Francoise Chauvin[1], & R.D. Astumian[2]. [1]Johns Hopkins Sch. Med., Baltimore, MD 21205 & [2]NHLBI, NIH, Bethesda, MD 20892.

A protein of a cell membrane is structurally sensitive to an electric field because of its charges, helix dipoles and polarizeability. Experiments showed that [Na,K]-ATPase of human erythrocyte could be induced to pump K^+ and Na^+ against their respective concentration gradient when the red cell was exposed to an oscillating electric field. The maximum stimulated activity was 20-30 ion per enzyme per sec at 3°C. The optimum voltage for both Na^+- and K^+-pumps was 20 V/cm, which could generate a $\Delta\psi$ of 12 mV, or a transmembrane electric field of 24 kV/cm. The optimum frequency differed for the two pumps, with 1.0 kHz for the K^+-pump and greater than 1 MHz for the Na^+-pump. No increased level of ATP hydrolysis was detected. Analysis based on a four state cyclic kinetic model indicates that an enzyme can capture free energy from an applied a.c. field for doing chemical work if the amplitude of the field matches the structure of the enzyme and the frequency matches the kinetic characteristics of the catalytic cycle. In the model, the essential steps are the field induced conformational transitions, through which energy is absorbed by the protein and transmitted to driving an endergonic reaction. Direct interaction between substrate and electric field is not required. Analysis also shows that certain enzymes are capable of modulating a stationary electric field to become locally oscillatory or fluctuating, thus, enabling them to transduce energy from a metabolism supported transmembrane potential. Mitochondrial ATPase belongs to this class and has been shown to undergo multiple turnover with a single d.c. pulse of 30 kV/cm, in the presence of 5 mM dithiothreitol.

(Supported by NSF Grant DCB 8611836 & an ONR contract to T.Y.T.)

Ref: Bioelectrochem. Bioenerg. 15, 457 (1986); Proc. Natl. Acad. Sci. 84, 434 (1987).

Th-AM-MinI-7 NA AND K CURRENTS IN BEATING HEART CELLS L. J. DeFelice, M. Mazzanti and D. Wellis, Anatomy and Cell Biology, Emory University School of Medicine, Atlanta, GA 30322

By averaging the current through a patch of membrane in a beating heart cell, and by monitoring the action potentials at the same time, we were able to study Na and K channels as they normally function. In 7-day chick ventricle cells in physiological solutions: (a) The fast Na channel has a dynamic reversal potential well below that in non-beating cells and significantly lower than the plateau of the action potential, which gives rise to a naturally occurring outward Na current during each beat. Because of the continual inactivation during diastolic depolarization, less than 10% of the available Na channels (23±21/μm2) are ever open at the same time. (b) During beating, the delayed-rectifier K channels have at least three conductance states: 60, 30, and 15 pS; all of these states have low densities (less than 10 channels/cell), and all have a -70 mV reversal potential and the same average kinetics. The -70 mV is an extrapolated potential. The dynamic K current never reverses, and no inward current flows through these channels during action potentials; the delayed-rectifier current follows the upstroke without appreciable delay and lasts the duration of the action potential. (c) The early-outward channel has a conductance between 18 and 9 pS depending on potential; it comes on immediately after the upstroke and conducts only during the first 50 msec of the action potential. The early-outward channel has an extrapolated reversal potential of -30 mV, but there is no inward current during beating. (d) The inward-rectifier channel in 1.3-2.5 mM external K has a conductance of 2-3 pS and no substates; it has an extrapolated dynamic reversal potential of -80 mV and conducts no outward current during the action potential. NIH HL27385-07 supports this work.

Th-AM-MinII-4 RAPID DETERMINATION OF LATERAL DIFFUSION COEFFICIENTS IN MODEL MEMBRANES USING ESR IMAGING. D. A. Cleary, Y.K. Shin, D.J. Schneider, and J. H. Freed, Baker Laboratory of Chemistry, Cornell University, Ithaca, New York 14853-1301

ESR Imaging has been used to rapidly determine lateral diffusion coefficients in oriented phospholipids. Diffusion coefficents D in the range of 10^{-8} cm^2 sec^{-1} have been determined in less than 1 hour. One dimensional concentration profiles in space were Fourier Transformed, and the decay of the Fourier components in time was analyzed to determine D. The rapidity of the method is based upon the high resolution permitting D to be accurately measured after a total diffusion distance of only ca. 100 microns. The method of analysis and several systems that have been studied will be discussed. The value of D has been determined as a function of temperature, type of lipid and percent added cholesterol for spin label 16PC and for cholestane (CSL). We find in the temperature range from 16° to 60°C, they ranged from 4 to 20 x $10^{-8}cm^2$/sec with activation energies found to be 6.3kcal/mole (CSL/POPC) and 8.6 kcal/mole (16PC/DMPC). Addition of cholesterol significantly decreases the values of D for diffusion of CSL (by about a factor of 2 for 10 mole % cholesterol). The implications for a free volume theory of diffusion in the bilayer will be considered.

Th-AM-MinII-5 IMAGING AND RELATED STUDIES BY ELECTRON SPIN RESONANCE - Minisymposium

H. J. Halpern[1], M. K. Bowman[2], G. M. Rosen[3], D. P. Spencer[3], L. A. Brunsting[3], J. Van Polen[1], T. D. Nguyen[1], B. A. Teicher[4], Y. Lee[4], A. C. Nelson[5].

[1]U. Chicago, Chicago, IL 60637, [2]Argonne, IL 60439, [3]Duke U. & VA Med Ctr. Durham, NC 27710, [4]DFCI, Harvard Med. Sch., Boston, MA 02115, [5]U. Washington, Seattle, WA 98105

The use of electron spin resonance requires the use of low frequency electromagnetic excitation to penetrate conducting, aqueous tissue. We have constructed an ESR spectrometer operating at 250 MHz with a 17ml sample holder capable of measuring spectra from spin label injected into live mice or spectra from spin label in the perfusate of whole organ preparations. The spectrometer includes imaging capability. In addition, we have developed a sensitive technique for measuring average oxygen tissue tension well suited for use in the spectrometer.

We will discuss the design of the spectrometer. We will demonstrate the spectrometer's capability for making measurements of spin label bioreduction in a whole organ preparation. We will present details of the oximetric technique using the low frequency spectrometer. We will demonstrate the use of this technique with measurements in live animals, and in measurements of tumors in vivo. We intend to present preliminary imaging studies with the spectrometer. Its potential for spin trapping studies will be discussed.

Th-AM-MinII-6 **L-BAND IN VIVO ESR**

M. J. Nilges, T. Walczak, and H. M. Swartz
University of Illinois, Illinois ESR Center, Urbana, IL 61801

Because of the lower dielectric loss of water at lower frequencies, ESR at L-Band (1-2 GHz) allows one to look at samples up to a few centimeters. We have designed a surface probe with a high Q and a resonant frequency of 1.1 GHz which not only allows us to look at samples on the order of a few centimeters, but allows us to probe into thick samples. Low frequency ESR allows us to follow the pharmacokinetics of nitroxide spin labels, particularly their redox metabolism. By the use of field gradients or by repositioning the probe, we can also monitor the distribution of nitroxides. Results are presented for tissue samples containing melanin and nitroxides and for live animals dosed with nitroxides.

Th-AM-MinII-1 ESR IMAGING MICROSCOPY OF BIOLOGICAL SAMPLES AT 9 GHz (X-BAND)

G. Bacic, T. Walczak, P. Morse II, F. Demsar, R. Woods, M. Nilges, J. Dobrucki, P. Lauterbur, H. Swartz
University of Illinois College of Medicine and ESR Center, Urbana, IL 61801

The purpose of these studies is to demonstrate the feasability of high resolution ESR imaging of biological samples at X-band (9 GHz) frequency. Two-dimensional data are obtained by use of two sets of computer controlled gradient coils, using filtered back-projection techniques for image reconstruction. Several applications of ESR imaging have been studied in both model and viable biological samples utilizing various nitroxide spin labels: 1) measurements of the distribution of oxygen and redox metabolism[1]; 2) fast imaging (less than 2min per 2D image) for diffusion studies[2]; 3) fat/water imaging in lipid-rich tissues exploiting the different solubilities of various nitroxides and/or oxygen in aqueous and lipid regions; 4) selective imaging of viable and nonviable (necrotic) regions in a tumor tissue model (spheroids). Images of melanin, the naturally occuring paramagnetic species in skin, also were obtained and may have implications for imaging of melanomas. Image resolution depends on the linewidths of the nitroxides that are used, but was generally sufficient (30-100 μm) to observe detailed structures of the sample. Very recently, three-dimensional ESR Imaging of model systems and some biological systems have been achieved.

[1]Bacic, et al. Magn. Reson. Med. Biol. 1 (1987) 000; [2]Demsar, et al., J. Magn. Resonance. (1988) in press. Partially supported by NIH Grant #RR01811.

Th-AM-MinII-2 IN-VIVO ESR AND EPR IMAGING, Lawrence J. Berliner, Hirotada Fujii, and Xiaoming Wan, The Ohio State University, Department of Chemistry, 120 W. 18th Avenue, The Ohio State University, Columbus, OH 43210

The promise of new methods of non-invasive detection of tissues, organs and physiological metabolites has come with the advent of magnetic resonance imaging (MRI) and in-vivo magnetic resonance spectroscopy. Most recently electron spin resonance (ESR) has been developed for in-vivo systems. While free radical processes in mechanisms of carcinogenesis and aging have been studied intensively in the past principally by in-vitro methods, we are now utilizing ESR spectroscopy for non-invasive detection of living animals. Due to the intense interest in nitroxides as potential NMR contrast agents (and built-in ESR imaging agents) we are currently studying the pharmacokinetics of nitroxides directly in-vivo, as a probe of redox metabolism in various tissues. The results are also promising in assessing the feasibility for ESR imaging measurements at the tissue site of interest. Supported by NIH grant RR03126 and the N.S.F. (DMB 8703794).

Th-AM-MinII-3 SPECTRAL-SPATIAL EPR IMAGING. **Martin M. Maltempo, Department of Physics, University of Colorado-Denver, Denver, CO 80202, Sandra S. Eaton, Department of Chemistry, University of Colorado-Denver, Denver, CO 80202, and Gareth R. Eaton, Department of Chemistry, University of Denver, Denver, CO 80208. (Intr. by Harold M. Swartz)**

Spectral-spatial EPR imaging gives the EPR spectrum as a function of position in the sample. Spectra are obtained at a series of static magnetic field gradients that correspond to projections in a spectral-spatial plane. For a given maximum magnetic field gradient, the spatial resolution of the image can be improved by collection of data for less than a full 180° angular range. We have used an iterative algorithm to estimate the "missing" information. Images have been obtained that show variations in nitroxyl lineshape due to collisional broadening and changes in motional averaging of the hyperfine interaction at different locations in the sample. The changing spatial distribution and the time-dependent variation in line shape through the sample are faithfully displayed in the two-dimensional spectral-spatial images. Three-dimensional images have been obtained with one spectral and two spatial dimensions. It is possible to get good spatial resolution along with good spectral resolution even when the display includes only portions of the spectrum of a paramagnetic metal.

Th-AM-A1 KINETICS OF INTERACTION OF CHROMATIUM AND CHLOROBIUM FLAVOCYTOCHROME c WITH SULFUR CONTAINING COMPOUNDS. M. A. Cusanovich and T. E. Meyer, Department of Biochemistry, University of Arizona, Tucson, AZ 85721.

Flavocytochrome c from the phototrophic bacteria is an unusual flavoprotein in that it contains both covalently bound heme and flavin. Electron transfer by flavocytochrome c occurs via the flavin moiety followed by intracomplex electron transfer to the heme moiety. Thought to be a sulfide dehydrogenase, flavocytochrome c reacts by a kinetically complex mechanism with a variety of mercaptans. With reactants like mercaptoethanol and cysteine, adduct formation between the flavin moiety and the mercaptan precedes heme reduction with at least one other intermediate required to describe the kinetic data. The kinetic mechanism with three different flavocytochromes c, from Chromatium vinosum, Chromatium gracile and Chlorobium thiosulfatophilum, has been characterized. The details of this unique reaction mechanism will be presented and the ramifications in terms of flavin chemistry will be discussed.

Th-AM-A2 RAPID CONVERSION OF SINGLY LIGANDED HUMAN CARBOXYHEMOGLOBIN TO A QUICKLY REACTING, LOW QUANTUM EFFICIENCY FORM. C. A. Sawicki and I. Zahroon. Physics Department, North Dakota State University, Fargo, ND 58105.

Carboxyhemoglobin solutions with less than 10% of the available heme sites bound to CO have been studied using stopped-flow/ laser photolysis. Statistical considerations suggest that $Hb(CO)_1$ should be the dominant liganded species present immediately following CO binding. Both the CO rebinding properties and the apparent quantum efficiency for photolysis of CO were observed to change dramatically during the first few seconds following CO binding. For example, in pH 7.0 kpi buffer at 20°C the apparent quantum efficiency for photolysis of CO was observed to change from near unity to 0.6 in a period of 2 seconds following the binding of CO. The quantum efficiency remained at 0.6 for at least an additional 30 seconds. Taking into account the slow rate of dissociation of CO from hemoglobin, the time dependence of the quantum efficiency appears to be inconsistent with description of changes in the CO binding properties of hemoglobin exclusively in terms of quaternary conformational changes.

Th-AM-A3 Ligand Binding Dynamics in Hb: Viscosity Dependence of Hemepocket Evolution and Properties of Rebound Heme Sites Subsequent to CO Photolysis.

E.W. Findsen[1], M. Chavez[1], J.M. Friedman[2], and M.R. Ondrias[1]
[1]Department of Chemistry, University of New Mexico, Albuquerque, NM 87131 and [2]AT&T Bell Labs, Murray Hill, NJ 07974.

Heme-protein dynamics have been demonstrated to play important roles in the ligand binding processes of hemoglobin (Hb). Resonance Raman scattering provides a specific and informative probe of the heme and its local environment. In this study, time-resolved resonance Raman spectroscopy was employed to trace the evolution of the heme active sites subsequent to CO photolysis from HbCO as a function of solvent viscosity and monitor the Fe-CO bond strength of religanded sites under solution conditions. Spectra were obtained from samples prepared with varying ratios of glycerol:water, buffered at pH 6.5 using previously established pump/probe protocols. The data obtained yielded the following insights into Hb ligand binding dynamics: 1) the initial proximal hemepocket geometry of the photolytic transient species is independent of solvent viscosity, 2) geminate ligand-heme rebinding does not appear to be influenced by solvent viscosity, while longer time rebinding is quite viscosity dependent, 3) the strength of the Fe-CO bond within 100 ns of religation is the same as that of equilibrium HbCO, and 4) relaxation of the metastable deoxy transient geometry is viscosity dependent, suggesting that it is predicated upon large-scale motions of the F-helix. Supported by the NSF (DMB8604435).

Th-AM-A4 LINEAR DIFFERENTIAL IMAGING MICROSCOPY OF ALIGNED INTRACELLULAR HEMOGLOBIN S POLYMER: THE EFFECT OF VARYING INTERNAL HEMOGLOBIN CONCENTRATION ON THE DOMAIN NUCLEATION AND GROWTH. J.D. CORBETT, Wm. Mickols, S.E. Embury, I. Tinoco Jr., M.F. Maestre, University of Cal., Berkeley, Lawrence Berkeley Laboratory, University of Cal., San Francisco.

Linear dichroism microscopy of sickled red blood cells determines the amount and orientation of aligned Hb polymer within the cells (Proc. Natl. Acad. Sci. USA, 82, 6527 (1985)). Sickle cells were incubated in hyper-, iso-, or hypotonic buffer solutions to change the internal hemoglobin concentration (MCHC). These cells were then sickled (using N_2) and fixed with glutaraldehyde. Images were analyzed for the percentage of aligned polymer in each cell and each cell was morphologically classified by the number and type of aligned polymer domains present.

The percent of aligned Hb and the number of domains in each class for each tonicity gave expected results in most cases when considering the effect of MCHC on polymerization using the double nucleation model of Ferrone et al. Increasing the MCHC caused an increase in number of domains while decreasing it caused many cells not to sickle and to have, unexpectedly, the same percentage of cells in some morphological classes (in cells that did sickle) as in the isotonic case. In the multiple domain class, the percent aligned Hb was smallest in the hypotonic case. We believe that these facts point to the possibility of preformed nucleation sites.

Preliminary results with Stractan density separations show a direct correlation between MCHC and the number of aligned polymer domains.

Th-AM-A5 FORMYL ISOTOPIC SUBSTITUTION AND HYDROGEN BOND SENSITIVE MODES IN HEME A MODEL COMPOUNDS: MODELS FOR CYTOCHROME A. Jose A. Centeno, Patricia M. Callahan[1], Juan Lopez-Garriga and Gerald T. Babcock*; [1]Departments of Chemistry, University of Nebraska, Lincoln, NE 68588, *Michigan State University, East Lansing, MI 48824-1322

To elucidate formyl (-CHO) modes in heme model compounds that mimic spectroscopic properties of cytochrome a in cytochrome oxidase, we have synthesized isotopically labelled Cu^{2+} porphyrin (-$CH^{18}O$), Cu^{2+} porphyrin a (-CDO), and heme a (-CDO), and characterized them by using optical absorption and resonance Raman (RR) spectroscopies. Resonance Raman activity of E_u-type IR-allowed substituent modes is observed. Upon substitution of ^{16}O with ^{18}O at the carbonyl group, the ν C=O stretching mode frequency decreases by 32 cm-1, and the ring-formyl stretching (ν Cb-CHO) *upshifts* by 4 cm^{-1}. The effect of hydrogen bond formation between the carbonyl group of heme a and phenol H-donors on Raman frequency shifts of formyl vibrational modes was also investigated. The $\Delta\nu$C=O and Δ^{ν}(max) values appear to be related to the pKa of the H-donor, but are insensitive to H/D exchange at the OH terminal end of the phenol H-donor group. In the *in situ* cyt a chromophore, H-bond sensitive vibrations were investigated under acidic denaturing conditions. The effects of acid pH on reduced cytochrome oxidase is to convert the high-spin cyt a_3^{2+} heme to a six-coordinate low-spin form as determined by loss of the 215 cm-1 and 1665 cm-1 and to shift the cyt a^{2+} formyl and vinyl group vibrations at 1612, 1397, 1334, 1247, 1228, and 658 cm-1. The resulting absorption and RR spectra resemble that of heme a^{2+} in a non-aqueous environment. The cyt a^{2+} band shifts and heme a formyl assignments presented here provide additional evidence for the strongly hydrogen bonded nature of the position 8 formyl group of cyt a in cytochrome oxidase. (Supported by NIH GM25480.)

Th-AM-A6 **Correlation between the Root-effect and variations of heme-distortions detected by resonance Raman scattering at hemoglobin Trout IV.**
R. Schweitzer-Stenner, D. Wedekind and W. Dreybrodt
University of Bremen, FB 1 - Physik, 2800 Bremen 33, F.R.G.

The depolarization ratio dispersion and the respective excitation profiles of two structural sensitive Raman lines of oxyhemoglobin-Trout IV (1375 cm^{-1} and 1638 cm^{-1}) have been measured at pH-values between pH = 6.5 and 8.6. They were analyzed by employing a fifth-order time dependent perturbation theory to calculate the Raman tensor. This provides information about the pH-dependence of parameters reflecting symmetry classified distortions of the prosthetic heme groups. In order to correlate these distortions with functional properties (Root-effect) the following protocol has been adopted: 1) A modified version of an allosteric model suggested by HERZFELD and STANLEY (J. Mol. Biol. 82, 231, 1974) has been applied to a set of oxygen binding curves of Hb-Trout IV (BRUNORI et al., Proc. Natl. Acad. Sci. USA 73, 4310, 1978). This provides information about the equilibrium constants of processes occurring upon oxygen binding, i.e. a) the T→R transition, b) protonation of Root- and Bohr-groups, c) coupling between quaternary and tertiary conformational states. 2) Assuming that each protonation state of the two quaternary conformations is related to a distinct set of symmetry classified heme distortions, a titration model is constructed which explains the experimental pH-dependence of the distortion parameters in terms of thermodynamic constants derived from the oxygen binding curves. This provides some interesting insights into the structural basis of the allosteric Root effect.

Th-AM-A7 NANOSECOND OPTICAL SPECTROSCOPY OF HEMOGLOBIN: COMPARISON OF GEMINATE REBINDING AND TERTIARY CONFORMATIONAL CHANGES IN THE R AND T QUATERNARY STRUCTURES. Lionel P. Murray, James Hofrichter, Eric R. Henry, Masao Ikeda-Saito, Keiko Kitagishi, Naoya Shibayama, Takashi Yonetani and William A. Eaton. Lab of Chemical Physics, NIDDK, NIH, Bethesda, MD 20892 and Dept. of Biochemistry and Biophysics, Univ. of Penn. School of Medicine, Philadelphia, PA 19104.

We have determined the effect of quaternary structure on the individual kinetic steps in the binding of carbon monoxide (CO) to the α and β subunits of hemoglobin. Time-resolved absorption spectra were measured after photodissociation of CO from a hemoglobin tetramer in which cobalt was substituted for iron in the β subunits or nickle was substituted for iron in the α subunits. The nickle and cobalt porphyrins do not bind CO. The results show that the liganded molecule, $\alpha(Fe\text{-}CO)_2\beta(Co)_2$, is in the R-state, and can be almost completely switched into the T-state by the allosteric effectors inositol hexaphosphate and bezafibrate. The geminate yield, or the probability that the ligand rebinds to the heme from within the protein, is found to be 40% for the R-state and less than 1% for the T-state. Within the simplest kinetic scheme, CO enters the protein in the R and T quaternary conformations at the same rate and the 60-fold decrease in the overall binding rate of CO to the subunit in the T-state compared to the R-state is almost completely accounted for by the decreased probability of binding after the ligand enters the protein. The results further suggest that the low probability for the T-state results from a decreased binding rate to the heme and not from an increased rate of return of the ligand to the solvent. Similar studies on $\alpha(Ni)_2\beta(Fe\text{-}CO)_2$ suggest the overall binding rate for the β subunits in the R and T states is also regulated by binding to the heme from within the protein.

Th-AM-A8 NANOSECOND SPECTRA OF TROUT I HEMOGLOBIN FOLLOWING PHOTODISSOCIATION OF THE CARBON MONOXIDE COMPLEX. Lionel P. Murray, Eric R. Henry, Massimo Coletta, James Hofrichter, Maurizio Brunori, and William A. Eaton. Laboratory of Chemical Physics, NIDDK, NIH, Bethesda MD 20892 and Department of Biochemical Sciences and CNR Center of Molecular Biology, University "La Sapienza", Rome, Italy.

Time-resolved optical absorption spectra in the Soret region have been measured following photodissociation of the carbon monoxide complex of component I of trout hemoglobin, as a function of temperature between 6 and 50° C. The experiment employs two Nd:YAG lasers producing 10 ns (FWHM) pulses for photodissociating and measuring spectra, as described previously (Hofrichter, et al., Biochem. 24, 2667 (1985)). Conformational changes in the deoxy photoproduct are monitored through changes in the deoxyheme optical spectrum. The photolyzed deoxy species exhibits two distinct spectral changes, which are assigned to tertiary and quaternary structural changes in the photolyzed molecule. The amplitudes of both spectral changes decrease markedly with increasing temperature. The yield for geminate rebinding of carbon monoxide to trout I hemoglobin decreases from 9% at 6° C to 3% at 50° C, whereas the rate for this relaxation is temperature-independent. Analysis of the rebinding data within a 3-species model indicates that both the rate of binding of carbon monoxide to the heme from within the heme pocket and the rate of escape of the ligand from the heme pocket into the solvent are essentially temperature-independent.

Th-AM-A9 STOCHASTIC MODEL FOR FLUCTUATIONS IN THE POLYMERIZATION OF SICKLE HEMOGLOBIN. Attila Szabo* (Intr. by S. Yoshikami) Lab. of Chem. Phys. NIDDK, NIH Bethesda, MD, 20892.

The time course of sickle hemoglobin polymerization is characterized by a marked delay, in which no polymer is formed, followed by an explosive increase in the amount of polymer[1]. This autocatalytic behavior can be understood in the framework of a double nucleation mechanism in which homogeneous nucleation is followed by heterogeneous nucleation on the surface of polymers formed via polymers formed via the first process[1]. Remarkably, it has been found[1,2] that the polymerization kinetics observed in very small volumes and in single cells can be irreproducible. This stochastic variability has been quantified in terms of a distribution of tenth times (i.e., the times at which the polymerization progress curves assume one-tenth of their limiting value) and has been attributed to fluctuations in the formation of single homogeneous nuclei.

Using the stochastic theory of chemical reactions and the theory of first passage times, we have derived a simple analytic expression for the distribution of tenth times expected on the basis of the double nucleation mechanism. This expression describes the shapes of the experimentally observed distributions very well and the rates of homogeneous nucleation obtained by least squares fitting the data agree with cruder estimates based on Monte Carlo simulations[2]. This work provides further support for the validity of the double nucleation mechanism and respresents a significant addition to the rather limited number of examples where contact can be successfully made between the stochastic theory of chemical kinetics and experiment.

[1]F.A. Ferrone, J. Hofrichter, W.A. Eaton, J. Mol. Biol. 183, 591, 611 (1985) and refs. therein.
[2]J. Hofrichter, J. Mol. Biol. 189, 553 (1986).

Th-AM-A10 METHYL REDUCTASE: COMPARISON OF RESONANCE RAMAN SPECTRA OF THE INTACT ENZYME AND F_{430} IN SOLUTION. J. A. Shelnutt[a], A. K. Shiemke[b], R. A. Scott[b], (a) Sandia National Laboratories, Albuquerque, NM 87185 and (b) University of Georgia, Athens, GA 30602

Methyl reductase of methanogenic bacteria catalyzes the reduction of 2-(methylthio) ethanesulfonic acid (methyl-S-CoM) to methane and HS-CoM. The methyl group of methyl-S-CoM ultimately comes from reduction of CO_2. Hydrogen is the source of reducing equivalents needed by the enzyme. The nature of the catalytic site of methyl reductase is of current interest from the point of view of developing biomimetic C_1 chemistry directed toward methane synthesis. We have obtained the first resonance Raman spectra of the nickel-macrocycle, called F_{430}, at the site of catalysis in intact methyl reductase. To help us structurally interpret the Raman spectra of the enzyme we also obtained Raman spectra of solutions of the major forms of F_{430} (salt-extracted and cytosol-free) at room temperature and at 77 °K and also, under similar solution conditions, spectra of a nickel-hydrocorphinoid derivative that is related to F_{430}. By analogy with the spectra of the model nickel-hydrocorphinoid, the F_{430} Raman spectra characterize the coordination of nickel(II) in F_{430} complexes, and provide some information about macrocycle ruffling. For the enzyme, the structure of F_{430} in the protein environment is found to be uniquely different from the F_{430} complexes and the F_{430} model-compound complexes that we have investigated to date. The Raman spectra of the enzyme are compatible with either 5- or 6-coordination although so far no ligands examined gives the high frequencies observed for the Raman coordination-state marker lines. Results of recent molecular modeling studies of F_{430} and its diepimer will also be presented.

Supported by the U. S. Department of Energy Contract DE-AC04-76DP00789 and the Gas Research Institute Contract 5082-260-0767.

Th-AM-A11 COORDINATION AND SPIN STATES OF FRESHLY PREPARED CYTOCHROME *c* PEROXIDASE, Siddharth Dasgupta and Denis L. Rousseau, AT&T Bell Laboratories, Murray Hill, NJ 07974; and Helen Anni and Takashi Yonetani, Department of Biochemistry and Biophysics, University of Pennsylvania, Philadelphia, PA 19104

The resonance Raman spectrum of cytochrome *c* peroxidase (CCP) in the ferric state shows that in freshly prepared enzyme the heme adopts a high spin, five-coordinate conformation independent of pH and the type of buffer. In aged enzyme, which is less stable, six coordinate high and low spin heme states are present. The addition of phosphate serves to stabilize the five coordinate form of the aged enzyme. Molecular modelling studies reveal that phosphate has access to a binding site near the heme and is capable of stabilizing the distal pocket, consistent with the experimental observations. In the ligand free ferrous enzyme the iron-histidine stretching mode at $247cm^{-1}$ decreases in intensity as the pH is increased. No shift in frequency of the line is detected as the pH is changed. Two different iron-carbon monoxide stretching frequencies are detected -- 535 cm^{-1} at low pH and a broader line at 505 cm^{-1} at high pH in the CCP-CO complex. These data may be interpreted as resulting from hydrogen bonding of the carbon monoxide to the distal histidine at low pH and a non-hydrogen bonded and relatively unconstrained carbon monoxide at the higher pH. The new results reported here bring the Raman scattering data into agreement with other spectroscopic and structural studies of this enzyme.

Th-AM-A12 RESONANCE RAMAN EVIDENCE FOR AN UNUSUALLY STRONG EXOGENEOUS LIGAND-METAL BOND IN A MONOMERIC NITROSYL MANGANESE HEMOGLOBIN. Shun-Hua Lin[#], Nai-Teng Yu[#] and Klaus Gersonde[+], [#]School of Chemistry, Georgia Institute of Technology, Atlanta, GA 30332, USA, and [+]Hauptabteilung Medizintechnik, Fraunhofer-Institut fur zerstorungsfreie Prufverfahren and [+]Fachrichtung Medizintechnik, Universitat des Saarlandes, D-6600 Saarbrucken, Germany (F.R.).

Resonance Raman spectroscopy has been employed to determine the vibrational modes of monomeric nitrosyl manganese Chironomus thummi thummi hemoglobin (CTT IV). This insect hemoglobin has no distal histidine. By applying various isotope-labeled nitric oxides ($^{14}N^{16}O$, $^{15}N^{16}O$, $^{14}N^{18}O$), we have identified the Mn-NO stretching mode at 628 cm^{-1}, the Mn-N-O bending mode at 574 cm^{-1} and the N-O stretching mode at 1735 cm^{-1}. The results suggest a strong Mn-NO bond and a weak N-O bond. The vinyl group substitution does not influence the ν(Mn-NO), the δ(Mn-N-O) and ν(N-O) vibrations. The Mn-NO stretching frequency is insensitive to distal histidine interactions with NO, whereas the N-O stretching frequency is sensitive. The above mentioned frequencies are insensitive to pH in the range of pH 5.1 to 9.3. However, a dramatic drop in intensity of the Mn-NO stretching was observed at pH 5.1. With the assistance of other spectral data this drop in intensity is interpreted as a transition of the hexa-coordinated to the penta-coordinated nitrosyl complex.

Th-AM-B1 A BESTIARY OF ION BINDING SITES IN PROTEIN CRYSTALS: CONTRIBUTIONS OF THE PEPTIDE BACKBONE AND LINEAR HYDRATION TO ION CHANNELS. G. Eisenman and A. Oberhauser. Introd. by W.F.H.M. Mommaerts. Physiol. Dept. UCLA Med. School, L.A. CA 90024 and Univ. of Pa. Phila. PA 19104.

Published refined Xray structures of 9 different protein crystals have been used for a molecular graphics examination (FRODO, PDV, MGRAPHIC) of 12 different binding sites for monovalent and divalent cations and 1 site for a divalent anion. The local hydration has also been studied. In this way a bestiary of ion binding sites and the channels giving access to them has been generated from which the contributions to ion binding and permeation can be assessed for backbone -C=O and -NH groups, side chain $-COO^-$ and side chain OH groups, as well as of local water molecules. Water molecules in refined structures are useful visual markers for sites and also give a clue as to potential low energy pathways to and from them. Such waters either complete the coordination of the cation or interpose themselves between the ion and a potential ligand. On occasion, the waters are seen to interact with a clearly defined path of backbone carbonyl oxygens that are appropriately oriented to serve as the lining of a narrow channel for ion (or water) movement. Water-ion-backbone interaction energies are probably comparable enough for the interchange of an ion and a water to occur at a reasonable rate. Complete charge neutralization locally is not required for binding. For example 1+ or 2+ charged cations can be bound to the same loops with 1 carboxylate in trypsin and subtilisin, divalent cations can be bound to E-F type Ca-binding loops with 1 to 4 carboxylates (the remaining ligands being carbonyls), and divalent sulphate can be bound by H-bonds to -NH's from the peptide backbone in the total absence of positively charged residues, cations or water. Charge delocalization underlying the ability to violate electroneutrality locally could be aided by H-bond interactions through chains of water molecules. Supp. by USPHS GM24749 and NSF BNS8411033.

Th-AM-B2 THE NATURE OF THE HYDROPHOBIC BINDING OF SMALL PEPTIDES AT THE BILAYER INTERFACE. Stephen H. White & Russell E. Jacobs, Dept. Physiology & Biophysics, University of California, Irvine, CA 92717.

We are studying the interactions of homologous series of hydrophobic peptides with lipid bilayers in order to refine and extend the usefulness of hydropathy plots. A particularly important issue is that of establishing the relationship between the thermodynamic transfer parameters of the peptides and their location within the bilayer phase. We report here partition coefficient and neutron diffraction measurements using hydrophobic tripeptides of the form Ala-X-Ala-O-t-Bu. ΔG_t, ΔH_t, & ΔS_t for the transfer of the tripeptides from water into DMPC vesicles were determined for X=Trp, Phe, & Leu. We find that $\Delta H_t = 0$ and $\Delta S_t > 0$ for all the tripetides above the phase transition of DMPC consistent with entropy-driven hydrophobic binding. Neutron diffraction measurements show that Ala-Trp(d_5)-Ala-O-t-Bu in oriented DOPC bilayers is located in the headgroup region. Thus, the tripeptides need not enter the hydrocarbon core for the hydrophobic effect to be seen. Plots of ΔG_t against a reference ΔG calculated from the accessible surface areas of the side groups reveals a linear relationship with a slope of 0.56 for X=Gly, Ala, Leu, Phe, & Trp. Trp is the most hydrophobic side group despite its polar character because its polar interactions remain satisfied at the interface. Supported by the NSF and the Am. Hrt. Assoc. REJ is an Established Investigator of the AHA.

Th-AM-B3 MAGAININ PEPTIDE STRUCTURE GOES FROM UNFOLDED TO HELIX UPON BINDING TO MEMBRANE SURFACE
Robert W. Williams*, Michael Zasloff^, and David Covell~, *Department of Biochemistry, Uniformed Services University of the Health Sciences, Bethesda, MD 20814, ~Department of Mathematical Biology, and ^Human Genetics Branch, National Institute of Child Health and Human Development, National Institutes of Health, Bethesda, MD 20892

Magainins are 23-residue peptides isolated from the skin of the african clawed frog. They protect the frog from infection under the most adverse circumstances and exhibit an extraordinary broad-spectrum antimicrobial activity in vitro [Zasloff (1987) Proc. Natl. Acad. Sci. USA 84, 5449]. This activity appears to involve the interaction of magainin with the microbial membrane. We have examined the mechanism of this interaction by correlating structural changes that occur when magainin and other peptides bind to membranes with properties of the peptide sequence. Raman spectroscopy of magainin 2 shows that it is 95% unfolded in physiological saline, and that it forms a 71% alpha-helix 14% turn structure upon binding to lipid vesicles. In comparison, melittin is 80% helix in solution and 83% helix bound to lipid. Magainin disrupts the acyl-chain region of DPPG lipid bilayers, but not to the extent observed for melittin. To quantitate the disruption of membrane bilayer by excess peptide, we have measured, at a temperature below the lipid phase transition, the intensity ratio of Raman bands corresponding to C-C stretching modes for cis and gauche conformers at 1062 and 1080 wavenumbers respectively. The results are expressed as an equilibrium constant, Kmelt = [I1080(+peptide) - I1080(pure unmelted vesicles)]/[I1062(+peptide) - I1062(pure melted vesicles)]. For magainin Kmelt = 0.11, while for melittin Kmelt = 4.2, indicating that magainin does not spontaneously span DPPG membranes. (Supported by USUHS GM7160)

Th-AM-B4 EFFECT OF MEMBRANE BINDING ON THE CONFORMATION OF ANGIOTENSIN II AND ITS ANALOGUES: A FOURIER-TRANSFORM INFRARED SPECTROSCOPIC STUDY. Witold K. Surewicz and Henry H. Mantsch
Division of Chemistry, National Research Council of Canada, Ottawa, Canada K1A OR6

Current hypotheses emphasize the role of lipid affinity and of lipid-induced peptide folding in peptide hormone-receptor interactions. Yet, very little is known so far about the conformational properties of peptide hormones in a lipid environment. We have used the technique of resolution enhanced Fourier-transform infrared spectroscopy to establish the conformation of the octapeptide hormone angiotensin II and that of some of its analogues. From the position of the conformation-sensitive amide I band it is inferred that in aqueous solution the majority of the backbone amide groups of angiotensin II are in a non-ordered conformation, with a fraction of these groups being involved in turn-like structures. While we find very little interaction between the peptide and the zwitterionic lipid phosphatidylcholine, binding to bilayers of the acidic phospholipid phosphatidylglycerol results in drastic conformational changes of angiotensin II. The lipid-associated hormone adopts a highly ordered secondary structure consisting of hydrogen-bonded beta-strands and turns. Whereas in aqueous solution some angiotensin II analogues adopt a conformation that is similar to that of the native hormone, in a lipid environment they fold into markedly different structures. These observations have important implications for the mechanisms of peptide hormone-receptor interactions and, particularly, for the postulated role of the lipid phase as a biologically important modifier of the hormone conformation.

Th-AM-B5 CHANNEL ION HELICITY AND INVERSE CYCLOTRON RESONANCE EIGENFREQUENCIES. A.R.Liboff, Dept of Physics,Oakland Univ,Rochester,Michigan 48309-4401, and B.R.McLeod, Elect Eng Dept, Montana State Univ,Bozeman,Montana 59717.

Membrane ion transport may be modulated by cyclotron resonance(CR) tuning in weak ($\sim 10^{-5}$ T) magnetic fields(Liboff,1985,Bull Am Phys Soc30,548). Originally suggested to explain the non-linear dependence of Ca^{2+} efflux from chick brain on low-frequency (16 Hz) modulated fields(Bawin et al, 1976,PNAS73,1999;Blackman et al,1985,Bioelectromagnetics6,327),there is now additional evidence for this phenomenon,derived from exposing cell culture to colinear magnetostatic and periodic magnetic fields(Smith et al,1987,Studia Biophysica119,131;Rozek et al,1987,Cell Calcium,in press). The calcium-dependent motility in diatoms(Amphora Coffeaeformis)exhibits resonance as a function of magnetic frequency with the maximum occurring precisely at the CR condition. We also find that ^{45}Ca-incorporation in human lymphocytes peaks sharply at a frequency (14.3 Hz) that is downshifted from the CR frequency corresponding to ^{40}Ca by the ratio of the isotopic masses, consistent with a q/m dependence. Despite this clearly observable CR signature, there is no small difficulty in invoking a CR mechanism: one must explain very long collision times (tens of milliseconds) and very low particle energies ($\ll$kT). Nevertheless, it is likely that the cell-field coupling occurs within channel proteins, for ions constrained to helical paths. It is thereby conceivable that certain ion channels in magnetic fields may exhibit associated low-lying energy states with corresponding harmonics of the fundamental CR frequency. Experimentally, we find that the motility of diatoms in magnetic fields tuned to the calcium charge-to-mass ratio does indeed peak at harmonics(1,3,5,15) of the fundamental frequency,supporting the idea of well-ordered helical motion for channel ions.

Th-AM-B6 **Intermembrane Protein Transfer** Alexandra C. Newton*and Wray H. Huestis†, *Department of Biochemistry, University of California, Berkeley, Ca. 94720 and †Department of Chemistry, Stanford University, Stanford, Ca. 94305

Bilayer-to-bilayer transfer of integral membrane proteins occurs when cells are incubated with liposomes composed of the relatively hydrophilic lipid, dimyristoylphosphatidylcholine (DMPC). Proteins transfer in functional form and in native orientation from the plasma membrane of erythrocytes and lymphocytes into the bilayer of sonicated vesicles. While the transfer is selective for certain proteins, the susceptibility of transfer appears to be unrelated to the hydrophobicity of the protein. Highly hydrophobic proteins (for example the erythrocyte anion transporter, band 3, with at least 12 transmembrane segments) as well as proteins purported to have only one transmembrane segment and a large extracellar domain (for example the viral glycoproteins of the murine lymphoma BL/VL3) are equally amenable to transfer. The insertion is spontaneous, reversible, and does not involve fusion, through solution transfer of solubilized protein, or association of membrane fragments with the liposomes. Bilayer destabilization resulting from incorporation of DMPC monomers into the cell membrane may promote protein transfer. A tentative mechanism is presented whereby apposition of cell and vesicle membranes, perhaps involving transient merging of the two outer monolayers, results in intermembrane transfer of integral plasma membrane proteins.

Th-AM-B7 THE ROLE OF NON-BILAYER PHASES IN THE LIPID TRANSFER BY LIPID EXCHANGE PROTEINS

Kwan Hon Cheng *, Marysue Mosgrober Anthony and Sek Wen Hui, * Departments of Physics and Biochemistry, State University of New York at Buffalo, Buffalo, New York, and Department of Biophysics, Roswell Park Memorial Institute, Buffalo, New York.

The rates of lipid transfer from small unilamelar vesicles of dimyristoylphosphatidylcholine (DMPC) to lipid mixtures of 1-palmitoyl-2-oleoyl-phosphatidylcholine (POPC) / dilinoleoylphosphatidylethanolamine (DLPE) in the presence of non-specific lipid exchange proteins from beef liver were measured. The rates of lipid transfer at 35 ^{o}C were determined for different molar ratios of POPC/DLPE as acceptors. A pronounced maximum in the transfer rate occurred when the POPC/DLPE started to exhibit non-bilayer structures in the form of bilayer disruptions and amorphous phases (intermediate phases) at PE greater than 80 %. The activity declined significantly when a majority of the lipids changed to the hexagonal phases. A similar observation was found when cholesterol or butylated hydroxytoluene (BHT) was present in the POPC/DLPE (2:8) mixtures. From the ^{31}P nuclear magnetic resonance and freeze-fracture electron microscopy measurements, both cholesterol and BHT were found to promote the hexagonal phases and inhibit the formation of intermediate phases in the POPC/DLPE mixtures. The extent of enhancement by cholesterol or BHT on the lipid transfer was lower than that by the addition of PE. This suggests that the presence of the intermediate phases is a major factor in modulating the activity of lipid exchange protein.

Th-AM-B8 LARGE 2-D CRYSTALS OF A MEMBRANE PROTEIN, VDAC, FORMED BY PHOSPHOLIPASE A_2 TREATMENT OF FUSED MITOCHONDRIAL OUTER MEMBRANES. Carmen A. Mannella, Wadsworth Center for Laboratories and Research, New York State Department of Health, Albany, New York, 12201.

The technique of slow lipid depletion by phospholipase/dialysis has been successfully applied to the 2-D crystallization of several membrane proteins. First success was achieved with the channel protein, VDAC, in the outer membrane of Neurospora mitochondria (mitOM) (Science 224:165, 1984). A limitation of the technique is that the maximum number of polypeptides per membrane crystal is apparently set by the number of polypeptides in each vesicle in the starting membranes. We have sought to increase the size of coherent 2-D crystals of VDAC (for electron crystallography) by membrane fusion. The fusion technique that works best with mitOMs involves slow drying at low pH (15 h under nitrogen at room temp., 5 mM KPi, pH 5). VDAC membrane crystals are typically cylindrical crystalline tubes, 0.25 μm wide and seldom longer than 0.4 μm. Best coherent fields (corresponding to one layer in a collapsed cylindrical array) contain at most about 600 unit cells. Fusion of pre-formed VDAC crystals leads to end-to-end joining of the cylinders in a non-coherent fashion. Instead, fusing the starting membranes produces round vesicles with larger collapsed diameters (1.5 μm vs 3-10 μm). Subsequent phospholipase A_2 treatment of the fused mitOMs yields well-ordered 2-D cylindrical crystals with widths of 0.4-0.5 μm and lengths of 1.0 μm or more. There is a 4-5-fold increase in the number of unit cells in the best coherent fields obtained after pre-fusion (approx. 3000). (Supported by NSF grant DMB 86-13702.)

Th-AM-B9 CHANNEL STRUCTURE OF AN OUTER MEMBRANE PROTEIN, PhoE PORIN. Bing K. Jap and Peter Walian (Intr. by Robert M. Glaeser), Donner Laboratory, Lawrence Berkeley Laboratory, University of California, Berkeley, CA 94720.

An outer membrane protein, PhoE porin, has been purified in trimeric form and reconstituted with phospholipid to form two-dimensional crystalline arrays. The crystal patches embedded in glucose give electron diffraction to a resolution of 3.4Å. The diffraction pattern shows strong reflections at about 4.0Å and about 10Å, indicating that the β-sheets are oriented approximately normal to the membrane plane. High resolution image reconstructions of PhoE porin embedded in glucose show high electron density regions indicating the locations of glucose-filled trimeric channels and of protein. The projected map suggests that PhoE porin consists of a hollow cylindrical structure of β-sheet of diameter about 28Å. Assuming that the cylindrical structure extends across the membrane, about 40Å thick, the number of β-strands needed to form such a hollow cylinder is about 19, each strand being 12 residues long. The total number of residues needed to form such a channel is about 230. Since PhoE porin consists of 330 residues, there are about 100 remaining residues for linker peptides and for forming a possible gating structure. This is consistent with our 3-D map of negatively stained PhoE porin obtained by electron crystallographic techniques to a resolution of better than 20Å . Our 3-D map shows trimeric channels, each of which is about 35Å long and 20Å wide. The trimeric channels traverse the membrane, but they do not merge. Each channel probably has an extended narrower segment that may play an important role in both its selectivity and gating mechanism.

Th-AM-B10 KINETICS OF MELITTIN-INDUCED FUSION OF PHOSPHOLIPID SMALL UNILAMELLAR VESICLES. Thomas D. Bradrick and Solon Georghiou, Biophysics Lab., Dept. of Physics, Univ. of Tennessee, Knoxville, TN 37996.

We have studied the kinetics of fusion of dipalmitoylphosphatidylcholine small unilamellar vesicles at 51°C which is induced by bee venom melittin at a lipid-to-melittin molar ratio of 60. This was done by following with a stopped-flow fluorometer the reduction in the ratio of the excimer to monomer fluorescence intensities of 1-palmitoyl-2-(10-pyrenyldecanoyl)-sn-glycero-3-phosphorylcholine (incorporated at 4 mol% into 9% of the vesicles) that accompanies fusion. At a low melittin concentration and low ionic strength, for which case the protein is monomeric, the value of the rate constant for fusion is 0.006 s^{-1}. This is much smaller than that of 0.06 s^{-1} obtained for a high melittin concentration at low ionic strength, i.e. for the protein in the tetrameric form which is not induced by a high salt concentration. The value of the rate constant for fusion for a low melittin concentration in the presence of 2 M NaCl, i.e. for the protein in the tetrameric form which is induced by a high salt concentration, is 0.12 s^{-1}. This is twice as large as that for fusion induced by the tetramer in a low ionic strength solution. These findings show that the state of aggregation of the protein in solution and, to a lesser extent, electrostatic interactions play an important role in the kinetics of melittin-induced fusion of vesicles. (Supported by NIH grant GM32433.)

Th-AM-B11 KINETICS OF MELITTIN BINDING TO PHOSPHOLIPID SMALL UNILAMELLAR VESICLES. K. Madhavi Sekharam, Thomas D. Bradrick and Solon Georghiou (Intr. by J.E. Churchich), Biophysics Lab., Dept. of Physics, Univ. of Tennessee, Knoxville, TN 37996.

We have used the shift in the fluorescence spectrum of the single tryptophan residue of bee venom melittin that accompanies binding to small unilamellar vesicles to determine the rate of binding through the use of stopped-flow fluorometry in the millisecond range. We have found the rate to depend on the length and the degree of saturation of the acyl chains as well as on the physical state of the bilayer and on the net electric charge of the polar groups. For dipalmitoylphosphatidylcholine, DPPC, the rate is maximal at the phase transition temperature T_t of the lipid, whereas for dimyristoylphosphatidylcholine, DMPC, it is maximal above T_t. The introduction of a double bond in each chain of DMPC results in a large increase in the rate. For a DPPC-to-melittin molar ratio of 100 the activation energies for binding below and above T_t are found to be about 9 and -11 kcal/mol, respectively. For zwitterionic lipids the rate-limiting step appears to be the partial penetration of the protein into the hydrophobic region of the bilayer. The rate decreases with a decrease in the lipid-to-melittin molar ratio, which suggests that the binding process exhibits negative cooperativity. For negatively charged lipids the results show that binding is a very fast process that appears to be electrostatic in nature. (Supported by NIH grant GM32433.)

Th-AM-B12 ITERATIVE CONVOLUTION ANALYSIS OF GAP JUNCTION X-RAY DIFFRACTION DATA. Thomas T. Tibbitts*, D. L. D. Caspar*, Walter Phillips* and Dan Goodenough+. *Rosenstiel Center, Brandeis University, Waltham, MA; +Harvard Medical School, Boston, MA.

Analysis of x-ray diffraction from isolated gap junction plaques is complicated by imperfect orientation of the stacked membrane pairs. Hexagonal packing of connexon channels within the plane of the membrane pair restricts the off-meridional diffracted intensity to relatively sharp lattice lines; however, these appear as smeared arcs due to the broad distribution of plaque orientations in the sample. For these data angular deconvolution cannot provide structure factors from overlapping equatorial and near-equatorial intensities. Our approach is to construct a three-dimensional model of the gap junction whose calculated crystal diffraction pattern, when convoluted with the appropriate disorientation function, closely resembles the observed pattern. A computer simulation and refinement procedure has been implemented to develop such a model. We begin with a trial three-dimensional structure based on information from electron microscopy and chemical composition measurements. Model structure factors are calculated and used to generate a diffraction pattern for comparison with the data. Ratios of observed-to-calculated intensities are used to adjust the model structure factors, subject to a minimum wavelength constraint. This cycle is repeated until the difference between the data and model pattern is minimized. Then the structure factors are transformed to produce an electron density map. This map is modified by application of structural constraints based on previous analyses of electron micrographs. A new set of structure factors is calculated and refinement against the data begins again. The analysis will be extended to higher resolution by building trial alpha helix and beta sheet into the refined low resolution structure.

Th-AM-B13 CORRELATION ANALYSIS OF GAP JUNCTION IMAGES. G.E. Sosinsky*, T.S. Baker+, D.L.D. Caspar*, and D.A. Goodenough++. *Brandeis University, Waltham, MA, +Purdue University, West Lafayette, IN and ++Harvard Medical School, Boston, MA.

Images of the connexon units in negatively stained and frozen-hydrated gap junction lattices have been averaged using both correlation and Fourier methods. The correlation averages were determined by selecting small portions of a Fourier-filtered image as reference, and then iterating the correlation by using the correlation averaged image as reference for the next cycle. For well-ordered lattices of connexons with uniform structure and orientation, such as those in frozen-hydrated specimens, the Fourier and correlation averages are quite similar. The correlation averages from lattices with irregularities, however, resolve details of the structure which are blurred in the Fourier average. Furthermore, many lattice images show local differences in orientation or staining of the connexon units and these differences can be distinguished by correlation procedures. Gap junction lattices which have been negatively stained show considerable variation in appearance due principally to variations in staining of the channel (Baker et al., J. Mol. Biol. (1985) **184**, 81-98). Cross-correlation maps show that connexons with large differences in axial staining are often irregularly distributed within a well-ordered lattice domain. In close-packed connexon lattice domains, the hexagonal connexon units are generally all skewed with the same hand, but correlation averages show that, in some cases, opposite orientations occur in different regions of single lattice. Correlation averaging provides a systematic method to correct lattice disorder and analyze local structural differences in periodic arrays.

Th-AM-C1 INHIBITION OF N-LINKED OLIGOSACCHARIDE TRIMMING AFFECTS GATING OF THE NICOTINIC ACETYLCHOLINE RECEPTOR IN BC3H-1 CELLS. M. Covarrubias, C. Kopta and J.H. Steinbach, Dept. of Anesthesiology, Washington Univ. School of Medicine, St. Louis, MO 63110.

Recent work has shown that inhibition of N-linked oligosaccharide trimming shifts the electrophoretic mobility of subunits of the nicotinic acetylcholine receptor (nAchR) expressed by BC3H-1 cells (Smith et al. 1986. J. Biol. Chem. 261: 14825-14832). We have studied the effects of sugar trimming inhibitors on the function of the nAchR using standard patch-clamp techniques. 1-deoxynojirimycin and castanospermine (1 mM and 25 μM respectively) reduced the number of surface receptors by 2-4 fold whereas the amplitude of the whole-cell current and the frequency of unitary currents were significantly more reduced (5-10 fold). This result suggested that the activation of the nAchR has also been altered. A more detailed analysis of the single channel properties in the low and high concentration limits of agonist concentration indicated that both the opening rate (β) and the rate of agonist dissociation (k_{-2}) were reduced by 2-3 fold, but the closing rate (α) and the single channel conductance were unaffected. This reduction in β is sufficient to account for the difference between the number of nAchR molecules on the surface and the physiological response (assuming an unaffected overall agonist affinity). In addition, upon treatment with 1-deoxynojirimycin the fraction of brief isolated openings (τ = 50 - 150 μsec) increased from 0.46 $\pm$ 0.04 to 0.61 $\pm$ 0.07 (fractions that remained constant over a 4 fold concentration range). None of these effects have been observed with swainsonine, which in contrast to the other inhibitors acts on a late enzyme of the processing pathway. In conclusion our observations suggest that early sugar trimming is important to express a normally functional nAchR on the cell surface (supported by NIH NS-22356).

Th-AM-C2 A SYNTHETIC PEPTIDE THAT MIMICS THE PREDICTED TRANSMEMBRANE M2 SEGMENT OF THE *TORPEDO* ACETYLCHOLINE RECEPTOR (AChR) δ SUBUNITS FORMS IONIC CHANNELS IN LIPID BILAYERS. S. Oiki*, W. Danho†, M. Montal*§, *Roche Institute of Molecular Biology, †Hoffmann-La Roche Inc., Roche Research Center, Nutley, NJ 07110, *§University of California San Diego, La Jolla, CA 92093.

A synthetic peptide, 23 residues long, with the sequence EKMSTAISVLLAQAVFLLLTSQR, corresponding to the putative transmembrane M2 segment of the *Torpedo* AChR δ subunit was incorporated into lipid bilayers. As shown in the figure, the synthetic peptide forms discrete channels in phosphatidylcholine bilayers. The most frequent event has a single channel conductance, γ=14 pS (0.5 M NaCl, 5 mM HEPES, pH 7.2; applied voltage 100 mV), one open state (τ_O=2.6ms) and two closed states (τ_{C1}=0.6ms, τ_{C2}=8.7ms).Events with smaller and larger γ were recorded at lower frequency of occurrence. Energetic considerations suggest that an aggregate of at least four amphipathic α helices conform channels. M2 exhibits high homology between subunits of the $\alpha 2\beta\gamma\delta$ complex and high evolutionary conservation among different species. Thus, the putative M2 segment may be a component of the AChR channel structure.

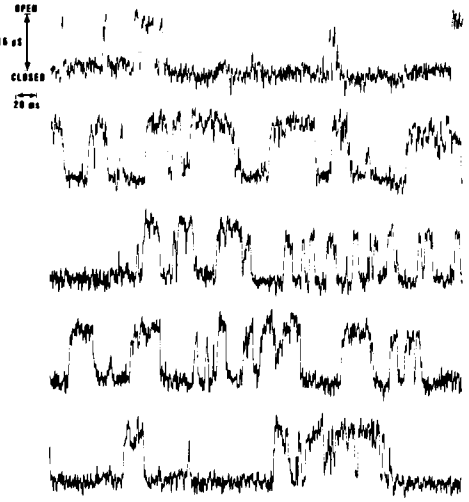

Th-AM-C3 **ELECTROPHYSIOLOGICAL PROPERTIES OF THE CLONED m1 MUSCARINIC RECEPTOR EXPRESSED IN A9 L CELLS.** S.V.P. Jones*, J.L. Barker*, T.I. Bonner+, N.J. Buckley+ and M.R. Brann[X]. *Laboratory of Neurophysiology, NINCDS; +Laboratory of Cell Biology, NIMH; [X]Metabolic Diseases Branch, NIDDK, National Institutes of Health, Bethesda, MD 20892.

The electrophysiological properties of A9 L cells transfected with the cDNA of the cloned m1 muscarinic receptor were studied using the whole-cell patch-clamp technique. Acetylcholine (50μM) elicited a hyperpolarization of the transfected cells but had no effect on non-transfected cells. Recordings under voltage-clamp revealed an outward current response at -50mV in the presence of acetylcholine, accompanied by an increase in conductance. The onset of the current response was consistently delayed by several seconds with respect to the onset of the application of acetylcholine, suggesting the involvement of a second messenger. The acetylcholine-induced currents were reversibly inhibited by 1μM atropine but were unaffected by 50μM tubocurarine. Ion substitution experiments, replacing potassium with N-methyl-D-glucamine and chloride with methyl-sulphonate determined that the current was carried mainly by potassium ions, although a small part of the current could be carried by chloride ions. The acetylcholine-induced current was inhibited when 5mM BAPTA was included in the patch pipette, suggesting the current was calcium-dependent. The acetylcholine-induced current could be blocked by a variety of potassium channel blocking agents, for example, TEA (20mM), 4-aminopyridine (3mM) barium (5mM) and apamin (0.5μM). Cobalt (5mM) and cadmium (100μM) also blocked the acetylcholine-induced current, providing further evidence of a calcium-dependent potassium conductance. Thus these results show that cloned m1 muscarinic receptors expressed in A9 L cells can activate a calcium-dependent potassium conductance, possibly via a second messenger system.

Th-AM-C4 GENETIC RECONSTITUTION OF FUNCTIONAL ACETYLCHOLINE RECEPTOR-CHANNELS IN MOUSE FIBROBLASTS. T. Claudio, W.N. Green, D.S. Hartman, D. Hayden, H.L. Paulson and A. Swedlund. Dept. of Cellular and Molecular Physiology, Yale University School of Medicine, New Haven, CT 06510

Foreign genes can be stably integrated into the genome of a cell using DNA-mediated gene transfer techniques, and large quantities of homogenous cells can then be isolated that continuously express these gene products. Such an expression system allows one to study the functional consequences of introducing specific mutations into genes, and also to study the expressed protein in the absence of the cellular components with which it is normally in contact. In this study, we succeeded in simultaneously introducing all four Torpedo acetylcholine receptor (AChR) subunit cDNAs into the genome of a mouse fibroblast cell using calcium phosphate coprecipitation, and a clonal cell line (all-11) was isolated. Although the copy number of the integrated cDNAs (4:2:2:8 for α, β, γ, δ, respectively) differed from the stoichiometry of the subunits found in AChR complexes (2:1:1:1), the cell line stably produced high concentrations of correctly assembled cell surface AChRs (12,000 per cell) that formed proper ligand-gated ion channels (see following abstract by Sine, et al.). The cell surface AChRs bound bungarotoxin with high affinity (K_D=7.8x10^{-11} M) and comigrated on sucrose gradients with precisely the same sedimentation coefficient as AChR isolated from Torpedo electric organ (9 S). Quite unexpectedly, we found that expression of Torpedo AChRs in mouse fibroblasts was acutely temperature sensitive. With this new stable expression system we will be able to combine for the first time, recombinant DNA, biochemical, pharmacological, and electrophysiological techniques to study Torpedo AChRs in a single intact system.

Th-AM-C5 FUNCTIONAL PROPERTIES OF TORPEDO ACETYLCHOLINE RECEPTORS GENETICALLY RECONSTITUTED IN MOUSE FIBROBLASTS. Steven M. Sine, Toni Claudio, and F.J. Sigworth. (Intr. by J. Hoffman) Dept. of Cellular and Molecular Physiology, Yale Univ. School of Medicine, New Haven, CT 06510.

Functional properties of Torpedo acetylcholine receptors were examined in a clonal mouse fibroblast cell line that had stably integrated the four Torpedo receptor cDNAs (all-11 cells; see Claudio, et al., previous abstract). The binding of agonists to intact cells was measured from their competition against ^{125}I-alpha-bungarotoxin binding. At steady-state, agonists show apparent dissociation constants of 0.7 uM for acetylcholine (Ach) and 10 uM for carbamylcholine. These dissociation constants are about 20-fold greater than those measured in Torpedo membranes, suggesting that receptors of all-11 cells more strongly favor the low affinity activatable over the high affinity desensitized state. The difference in dissociation constants can be accounted for by a ratio of desensitized to activatable receptors of 10^{-4} for all-11 cells compared to a ratio of 10^{-1} for Torpedo membranes. Patch clamp techniques were used to record currents through single receptor channels of all-11 cells. In "outside-out" patches, no currents were seen in the absence of agonist, but intense channel activity was seen following bath application of 1 to 5 uM Ach. The single channel conductance is 29 pS in sodium Ringer solution at 15°C. At low concentrations of Ach (1-2 M), channel openings appear largely as open and shut events, but are occasionally interrupted by brief closings. Analysis of the low concentration measurements discloses estimates of the channel closing rate (2000 s^{-1}), the channel opening rate (2500 s^{-1}), and the agonist dissociation rate (30000 s^{-1}), at a potential of -60 mV and 15°C. Both the conductance and the channel gating parameters agree closely with those obtained from Xenopus oocytes injected with mRNA coding for the four Torpedo receptor subunits.

Th-AM-C6 M-CURRENT SUPPRESSION BY AGONISTS: THE ROLE OF THE PHOSPHOLIPASE C PATHWAY. P.J. Pfaffinger, M.D. Leibowitz, M.M. Bosma, W. Almers, and B. Hille. Physiol. & Biophys., Univ. of Wash., Seattle, WA 98195.

We have examined the roles of the phospholipase C pathway second messengers (internal Ca, IP_3, and protein kinase C) in the suppression of M-current by agonists. Enzymatically isolated frog sympathetic neurons were studied by whole-cell voltage clamping while internal free Ca was measured with the Ca indicator FURA 2. With 50 μM FURA 2 in the recording pipette and no additional Ca buffer, the steady-state intracellular Ca concentration was 20-60 nM at -35 mV. Addition of t-LHRH, muscarine, or substance P (SP) suppressed M-current and produced a transient (30-100 nM) increase in free Ca. The Ca rise is due, in part, to release from internal stores: first, a small Ca rise was seen with 0 external Ca; second, the Ca transient was reduced or absent with repeated muscarine or t-LHRH applications suggesting a depletion of Ca stores. The M-current remained agonist sensitive with 1 mM EGTA or 5 mM BAPTA in the pipette, but the Ca transient was reduced or unmeasurable under these conditions. Further, raising internal Ca to >200 nM (a concentration greater than that elicited by agonists) or including 100 μM IP_3 in the pipette solution had no effect on the M-current or on its suppression by transmitters. Activation of protein kinase C with 1 μM PMA does suppress M-current by 50%, but this suppression cannot be further enhanced by raising internal Ca or IP_3 levels. Subsequent addition of t-LHRH always suppressed the remaining M-current completely and reversibly. These results suggest that while agonists that suppress M-current may activate phospholipase C, the IP_3 and Ca pathways are unimportant for suppressing M-current, and protein kinase C activation is unable to produce a full suppression; therefore, other messenger systems must also be involved in the normal agonist response. Protein kinase C activation may play some role in desensitization of SP responses. Single applications of SP cause a complete suppression of M-current. However, this suppression is transient, and subsequent responses to SP are dramatically reduced or absent. t-LHRH responses remain normal suggesting a specific desensitization of SP receptors. Pretreatment with 1 μM PMA prevents suppression of M-current by SP, mimicking desensitization. Supported by NIH grants NS08174, AR17803. M.D.L. is a FESN scholar in transduction of neuronal signals.

Th-AM-C7 TWO FUNCTIONAL TYPES OF EXCITATORY AMINO ACID RECEPTOR SYNTHESIZED FROM RAT BRAIN mRNAs. T.M.Fong, N.Davidson, & H.A.Lester, Divs of Biol & Chem, Calif Inst of Tech, Pasadena, CA 91125.

Poly(A)$^+$ mRNAs from rat brain or rat hippocampus were injected into Xenopus oocytes, and functional excitatory amino acid (EAA) receptors were studied by voltage-clamp method. One type of receptors, EAA receptor/channel, is characteristic of ligand-gated cation channels. The inward current response is fast and smooth, and it can be activated by NMDA (up to 200 nA) or kainate (up to 600 nA), or high concentration of L-glutamate or quisqualate. The second type of receptors, EAA receptor/transducer, is characteristic of membrane receptors coupled to Ca^{++}-activated Cl^- channel through intracellular second messenger (G protein and IP_3). The inward current response is delayed, oscillatory and desensitized rapidly, and it can be activated by L-glutamate or quisqualate (up to 500 nA), or high concentration of NMDA. DL-AP5 or D-α-AA inhibits the EAA receptor/channel activated by either NMDA or kainate, but not the EAA receptor/transducer (with 10 mM of antagonist). Dose-response analyses revealed that the activation of EAA receptor/channel required the highly cooperative binding of two agonist molecules. The K_d for NMDA is 80 μM, as compared to kainate K_d of 0.01 μM. Glycine binds to only one of the two sites with a K_d of 0.5 μM, which explains why micromolar level of glycine can potentiate the NMDA response but not the kainate response. The mRNAs were further size-fractionated to study the molecular composition. About 20-fold purification in specific activity (nA/ng of mRNA injected) of mRNAs encoding the EAA receptor/transducer has been achieved. In contrast, significant purification of the mRNAs encoding the EAA receptor/channel has not been successful, which suggests that it may be encoded by multiple species of mRNAs. (Supported by MDA fellowship, NIH grants NS11775 & GM10991).

Th-AM-C8 DESIGN OF PEPTIDE TOPOLOGY VIA SYNTHETIC INCORPORATION OF CONFORMATIONALLY RESTRICTED AMINO ACIDS, BIASED TOWARDS GAUCHE+, TRANS OR GAUCHE- SIDE CHAIN CONFORMATION. W. Kazmierski and V.J. Hruby, Department of Chemistry, University of Arizona, Tucson AZ 85721 U.S.A.

We have synthesized four analogues of the cyclic octapeptide Xxx-Cys-Tyr-D-Trp-Orn-Thr-Pen-Thr-NH_2, which incorporate conformationally restricted amino acids at the N-terminal position critical for affinity to mu opioid receptors. 2 is derived from 1 by bridging the amino and o-aromatic moieties of 1 with a methylene group. 3 is similar to 2, except that the C-C ortho bond is now disconnected. ^1H NMR and computer modeling studies have demonstrated that while 1 has the; g^+, g^-, and t side chain conformers all present, 2 exists exclusively in g^-, and 3 is mostly trans. 4 exists exclusively with a g+ side chain conformation as a result of a dramatic conformational change in 4 upon coupling of glycine to 2. These results correlate well with the biological data. Peptide II is the most μ opioid receptor specific legand known. I, III and IV exhibit much weaker affinity for mu opioid receptors. Other conformational investigations suggest that it is mainly different conformational biasing of the position 1 amino acids in analogues 1-4 which determines mu opioid receptor selectivity, with the g^- conformation (but not g+ or t) especially relevant for binding to the μ receptor. Thus, unique insights into the topological structural requirements for receptor recognition in general can be obtained by this approach.

Xxx	aminoacid entry	peptide entry
D-Phe	1	I
D-Tic	2	II
D-N-MePhe	3	III
Gly-D-Tic	4	IV

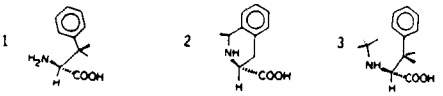

Th-AM-C9 ROTATIONAL DIFFUSION AND MICRO-AGGREGATION OF FLUORESCENCE-LABELED ACETYLCHOLINE RECEPTORS ON LIVING MUSCLE CELLS IN CULTURE. Marisela Velez and Daniel Axelrod, Biophysics Research Division and Dept. of Physics, University of Michigan, Ann Arbor, MI 48109

Acetylcholine receptors (AChR) on rat myotubes in primary culture occur in two coexisting states of aggregation: localized clusters of several hundred square microns consisting of hundreds of submicron microclusters; and predominately nonclustered regions elsewhere. To examine how such AChR clustering is organized and controlled, we have examined AChR (labeled by rhodamine bungarotoxin) in both types of regions by two novel fluorescence techniques: polarized fluorescence photobleaching recovery (FPR) for measuring receptor rotational diffusion; and scanning fluorescence correlation spectroscopy (FCS) for measuring the degree of receptor aggregation. Polarized FPR on living cells requires automated sample translation, signal averaging, and two sets of recovery curves corresponding to orthogonal bleaching polarizations. Scanning FCS requires data to be gathered with both small and large observation areas (set by an image plane diaphragm) scanned through the same raster pattern, to distinguish rapid fluctuations arising from AChR microclusters from slower fluctuations arising from background variations. From polarized FPR, we find that the AChR in clustered regions are rotationally immobile, whereas thosein nonclustered regions are rotationally mobile with an average diffusion coefficient around 200 sec^{-1}. This rate tends to decrease with myotube age. From scanning FCS, we find that the average microcluster in clustered regions consists of several hundred aggregated AChR. Supported by an American Association of University Women Fellowship and US PHS NIH grant #NS14565.

Th-AM-C10 DISPOSITION OF ALPHA-TOXIN ON THE SURFACE OF THE NICOTINIC ACETYLCHOLINE RECEPTOR: FLUORESCENCE DIPOLAR ENERGY TRANSFER AND QUENCHING STUDIES. **David A. Johnson and Rosemary Cushman*, Division of Biomedical Sciences, University of California, Riverside, CA 92521.**

Four mono-fluorescein isothiocyanate derivatives of cobra alpha-toxin (Naja naja siamensis 3) were isolated and the sites of labelling were determined to be at the N-epsilon amino groups of lysines 23, 35, 49 and 69. Bimolecular quenching rate constants derived from the Stern-Volmer iodine quenching constants and fluorescence lifetimes indicated that the fluorophores were solute accessible both when the derivatives were free in solution and bound to the Torpedo acetylcholine receptor. Dipolar energy transfer from the receptor tryptophanyl residues to the bound alpha-toxin derivatives was 50% greater to the lys-49 derivative than to the other three derivatives examined. Energy transfer was measured between the four fluorescein derivatives and mono-tetramethylrhodamine-N-epsilon-lysine-23-alpha-toxin bound to the membrane-associated and detergent solubilized acetylcholine receptor. Greater specific energy transfer was observed with the membrane-associated receptors confirming that transfer between fluorophores on separate receptors molecules is greater than that occurring intramolecularly between the two sites on the receptor. The relative magnitudes of the specific energy transfer between the fluorescein and tetramethylrhodamine derivatives provide additional constrains to models for the disposition of alpha-toxin on the surface of the acetylcholine receptor.

(Supported by US Army Medical Research and Development Command, contract N. DAMD 17-84-C-4187.)

Th-AM-C11 BETA SUBUNIT OF MOUSE-TORPEDO HYBRID ACETYLCHOLINE RECEPTORS EXPRESSED IN XENOPUS OOCYTES DETERMINES SENSITIVITY TO A NON-COMPETITIVE INHIBITOR. R.J. Leonard, C. Labarca, N. Davidson, and H.A. Lester. Division of Biology, Caltech. Pasadena, CA. 91125.

One strategy for examining structure-function relationships of the nicotinic acetylcholine receptor (AChR) is to study the effects of structural changes on the activity of non-competitive inhibitors (NCIs), since the primary site of action of many NCIs appears to lie within the ion channel of the AChR. We have been using the compound N-p-phenyl-azo-phenyl-carbamylcholine (EW-1) which acts as a light-activated open channel blocker on synaptic AChRs at the Electrophorous electroplax.

Oocytes were injected with AChR subunit mRNAs transcribed in vitro from cDNAs of mouse BC3H1 cells or Torpedo electric organ to express "MOUSE", "TORPEDO", or "HYBRID" (mixtures of subunit mRNAs from both species) AChRs in their plasma membranes. Oocytes were voltage-clamped and subjected to voltage jumps and light flashes in the presence of 0 to 1 uM ACh and the effect of EW-1 on the resultant current relaxations was examined.

For "MOUSE"-type AChRs, 1 uM trans-EW-1 had no effect on the ACh-induced currents at all voltages. Flash isomerization (trans->cis) of the EW-1 caused a reversible, voltage dependent decrease in the ACh-activated currents, as though the flash created a transient increase in the concentration of open channel blocker.

"TORPEDO"-type channels, however, were blocked >90% by the trans isomer of EW-1, and the effect of flash isomerization to the cis form was to relieve the block at positive voltages.

The sensitivity to trans-EW-1 in "HYBRID" AChRs was determined by the source of the beta subunit. By titrating the EW-1 concentration, both flash-activated blocking and unblocking could be observed in "Torpedo"-like HYBRIDS, but unblocking was not observed in HYBRIDS which contained a beta subunit from MOUSE. The effect of beta subunit on sensitivity to QX-222 appears to follow the same pattern. Supported by NS-11756 and an MDA fellowship.

Th-AM-C12 STRUCTURAL MODEL OF THE GABA RECEPTOR CHANNEL

H. Robert Guy and G. Raghunathan, Lab. Math. Biology, NCI, NIH, Bethesda, MD 20892

A three dimensional model of the GABA receptor's transmembrane region was developed from sequences determined by and transmembrane topology proposed by Schofield et al.(1987, Nature 328:221). In this model four transmembrane α helices (M1-M4) from each subunit form a bundle of antiparallel α helices with 3-4 ridges-into-grooves packing (see figure). The channel is postulated to be formed by a dimer consisting of one A subunit and one B subunit. The pore is in the center of a bundle of four α helices (M1A, M2A, M1B, and M2B) that also has 3-4 ridges-into-grooves packing. The pore is lined primarily by serine and threonine residues and is just large enough to pass the larger permeant anions. Arginine side chains near both entrances and a histidine side chain at the extracellular entrance make the channel anion selective. M1 and M2 sequences are highly conserved when comparing A and B subunits of the GABA receptor to each other or to the B subunit of the Glycine receptor whereas M3 and M4 exhibit "unilateral conservation" in which one face of the helices is conserved while the opposite face has many substitutions. The poorly conserved faces of M3 and M4 are hydrophobic and are postulated to be in contact with lipid. The well conserved faces of M3 and M4 contain primarily phenylalanine and tyrosine side chains that pack between each other on adjacent M1 and M2 α helices. Channel gating may involve cooperative interactions between dimers.

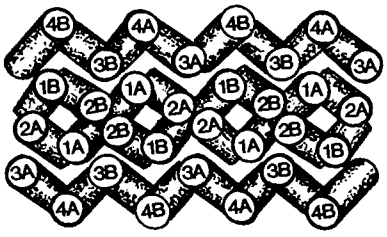

HELICES OF FOUR GABA RECEPTORS

Th-AM-C13 PROPERTIES OF KAINIC ACID INDUCED Ca^{2+} TRANSIENTS IN SINGLE STRIATAL NEURONS

S.N. Murphy, S.A. Thayer, and R.J. Miller, University of Chicago, Chicago, IL 60637 (Intr. by G.A. Jamieson)

It has been suggested that increases in $[Ca^{2+}]_i$ may underlie kainic acid (KA) induced neurotoxicity. Therefore we have examined the effects of KA in monolayer cultures of striatal neurons using fura-2 microfluorimetry. 50 mM potassium, 10 μM veratridine, 100 μM KA and 30μM amino-3-hydroxy-S-methyl-4 isoxazoleproprionate (AMPA) were applied by perfusion. $[Ca^{2+}]_i$ was measured during multiple 5 minute applications for up to 40 minutes. All stimuli raised $[Ca^{2+}]_i$ to similar peak values. However, KA and AMPA often caused $[Ca^{2+}]_i$ oscillations with a period of ~ 2 minutes. When KA or AMPA was applied to the same cell a second time the increase in $[Ca^{2+}]_i$ was attenuated 30-80%. Neither of these properties were observed during depolarization with 50 mM K^+ or 10 μM veratridine. None of the stimuli caused changes in $[Ca^{2+}]_i$ in Ca^{2+} free media. Voltage sensitive calcium channels contribute to the KA response as inactivatation of Ca^{2+} channels by predepolarization (50 mM K^+) in Ca^{2+} free media in the presence of 1 μM Nitrendipine attenuated KA induced increases in $[Ca^{2+}]_i$ by >90%. Increases in $[Ca^{2+}]_i$ due to 50 mM K^+ or 10 μM veratridine were also attenuated by >90% by predepolarization with 50 mM K^+ and 1 μM Nitrendipine. In preliminary studies using the whole-cell patch-clamp technique we have found these striatal neurons to have L, N, and T type currents as previously described in peripheral neurons. Typical peak N-type currents of 250 pA's were found as compared to peak L-type and T-type currents of < 40 pA's.

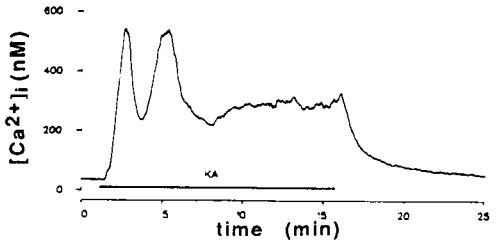

Th-AM-D1 VOLTAGE SENSITIVE DYE RECORDINGS FROM INTACT HEARTS USING OPTICAL FIBERS

SM Dillon & AL Wit. Columbia Univ., Department of Pharmacology, NYC, NY.

Voltage sensitive dyes hold the promise of allowing optical recordings of cardiac action potentials (APs) under conditions which preclude the use of microelectrodes such as: a) large numbers of simultaneous recordings, b) contracting heart or c) inaccessible areas (ex. inside ventricle). The cardiac laser scanner (Dillon & Morad, Science 214:453,1981) was the first development to allow large numbers of optical AP recordings. To date, however, conditions b) & c) have stymied optical methods as well. Care must be taken to pharmacologically or mechanically limit cardiac movement in order to reduce signal distortion and spatial inaccuracy. In addition, since current techniques rely upon direct line of sight between the heart and instrumentation, complete exterior coverage is difficult and internal coverage impossible. These problems are resolved through our use of optical fibers to carry light back and forth between a recording site on the heart and the instrumentation. Optical fibers, fixed in place, eliminate inaccuracies caused by heart movement while the "light piping" property allows recordings to be made from any site accessible to the fibers. A simple 2 fiber configuration uses one fiber to deliver optical excitation and another fiber to return the dye signal to a photodetector. We have also used single optical fibers to carry both excitation and optical signal and are presently employing this approach to implement a multiple site optical AP recording system.

Th-AM-D2 **A NOVEL CARDIAC POTASSIUM CHANNEL THAT IS ACTIVE AND CONDUCTIVE AT DEPOLARIZED POTENTIALS**

David T. Yue and Eduardo Marban,
Division of Cardiology, Johns Hopkins Hospital, Baltimore, MD 21205

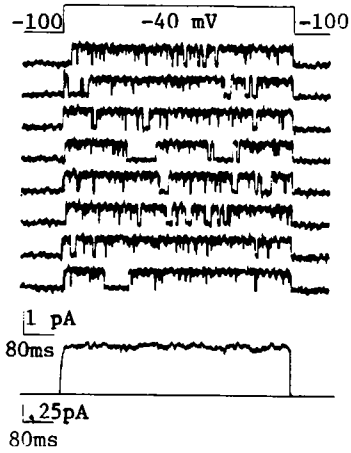

We report the existence of a novel potassium channel revealed in single-channel recordings from guinea pig ventricular heart cells. The channel, observed in ~10% of patches, demonstrates a 14 pS conductance at physiological potassium concentrations, does not rectify over the voltage range of the action potential, and is quite selective for K ions. Sequentially obtained current records are displayed on the left in response to the diagrammed voltage protocol. The channel activates with depolarization, but does not require intracellular Ca^{2+} ions to open. Open channel probability increases rapidly (<10 ms) to a plateau in response to depolarizing voltage steps, and demonstrates no detectable inactivation (>600 ms) [see ensemble average at left]. Because of these features, this channel, in contrast to other known cardiac K channels, seems particularly suited to carry the predominant share of outward current during the plateau of the action potential in heart muscle. Accordingly, we designate the channel i_{Kp}.

Th-AM-D3

CYTOSOLIC CALCIUM TRANSIENTS FROM THE INTACT MAMMALIAN HEART.

Hon-Chi Lee, Rajendra Mohabir, & William T. Clusin. Cardiology Division, Stanford University School of Medicine, Stanford, CA 94305.

We have developed a method of recording cytosolic calcium transients from isolated rabbit hearts. Intracellular loading of indo-1 was accomplished by retrograde coronary perfusion with indo-1 AM (2.5 μM) for 30 min. at 30°C, followed by 30 min of wash-out. Hearts were illuminated at 360 ± 5 nm through a fiberoptic cable onto the left ventricular epicardial surface. Fluorescence emissions were collected by a ring of 8 coaxial fiberoptic cables, divided by a beam splitter, and recorded simultaneously at 400 ± 12.5 nm and 550 ± 20 nm. The F400/F550 fluorescence ratio was calculated by an analog circuit which allowed cancellation of small motion artifacts. Indo-1 loading produced a 5 to 12 fold increase in fluorescence at both emission wavelengths, without impairment of contraction or relaxation. The $[Ca^{2+}]_i$ transients demonstrated rapid upstrokes, which preceded the onset of contractions, and slow decays, which often continued after mechanical relaxation was complete. The peak amplitude of the $[Ca^{2+}]_i$ transients was increased by ouabain, adrenaline, post-extrasystolic potentiation, and acetylcholine. Adrenaline also produced acceleration in the decay of the $[Ca^{2+}]_i$ transients, along with faster mechanical relaxation. Perfusion with caffeine impaired both $[Ca^{2+}]_i$ and mechanical relaxations. Ischemia produced a marked increase in both the peak-systolic and end-diastolic $[Ca^{2+}]_i$, which approached plateau values after 90 sec. Reperfusion promptly restored $[Ca^{2+}]_i$ to baseline levels. These observations are consistent with a proposed role of $[Ca^{2+}]_i$ in mediating electrophysiological abnormalities during early ischemia.

Th-AM-D4 QUINIDINE BLOCKS THE INWARD-RECTIFIER K+ CHANNEL (IK_1) FROM THE INSIDE OF THE MEMBRANE IN GUINEA PIG VENTRICULAR MYOCYTES. R Sato, I Hisatome, JA Wasserstrom, DH Singer, Reingold ECG Center, Northwestern University, Chicago, IL.

Quinidine slows the rate of action potential repolarization and reduces resting potential. These actions are thought to reflect reduced K^+ permeability. However, this has not yet been documented by direct measurements of quinidine effects on K^+ channel activity. We, therefore, studied the effects of quinidine on IK_1 in isolated guinea pig ventricular cells using single channel recording techniques (inside-out patch). The pipette solution contained (in mM) 140 KCl and 5 HEPES (pH 7.4). The internal solution contained (in mM) 120 K aspartate, 3 Na_2ATP, 5 EGTA, 5 HEPES, 1 $MgCl_2$. To analyze channel gating behavior, we fitted channel open and closed times to probability density functions. The open time histograms could be fitted by a single exponential curve; the closed time histograms, by two exponential curves. These results suggest that the channel has two closed states and one open state. Under inside-out patch conditions, the current-voltage relationship showed that E_K was close to 0 mV and inward channel conductance was 40 ± 4 pS (n=4). When we superfused the cell with an internal solution containing quinidine (30 μM), the open probability decreased. Within 3 minutes, unit conductance decreased from 40 ± 4 pS to 20 ± 3 pS (n=4). Channel activity was completely suppressed after 5 minutes. Channel activity reappeared following washout for 5 minutes suggesting that quinidine's blocking effects were reversible. In summary, our results demonstrate that quinidine blocks Ik_1 by reducing both open probability and unit conductance. These actions could underlie both the slowing of repolarization of the action potential and the reduction of the resting potential by quinidine.

Th-AM-D5 **LANTHANUM-SENSITIVE CURRENT CONTAMINATES I_K IN GUINEA PIG VENTRICULAR MYOCYTES.** Jeffrey R. Balser, Dan M. Roden. Vanderbilt Univ., Nashville, TN.

Multiple transmembrane currents contribute to the net current that develops during prolonged depolarization in heart. We have used the whole cell configuration of the patch clamp method to study the delayed rectifier (I_K) in disaggregated guinea pig ventricular myocytes. Tyrode's was first altered to eliminate I_{Na} and I_{si}: Na_o was replaced with equimolar Tris, and 0.1 mM Cd_o was added to block the L Ca channels. Ca_o was reduced to 0.1 mM and Mg_o raised to 2 mM. An "envelope test" was then performed: the time course of current activation at +50 mV was compared to the time course of current tail amplitudes at -30mV after steps of variable duration to +50mV. In altered solutions, the envelope test was not satisfied (figure, top) with scaled tail amplitudes developing faster than scaled activating current (n=6). Therefore, measurements of I_K in these solutions were contaminated by another current. However, with altered solution + La^{3+} (10-100 μM, n=3 [paired]; ≥ 30 μM, n=3 [unpaired]), tail amplitude development slowed, activating current time course was unaltered, and the envelope test was satisfied (figure, bottom). Similarly, the envelope test was not satisfied in Tyrode's alone, but was improved in Tyrode's + La^{3+}. These data suggest the presence of a La^{3+}-sensitive, Cd^{2+}-insensitive current in these preparations that is apparent in deactivating current tails following strong depolarizations. La^{3+} may be useful as a tool for studying I_K in isolation.

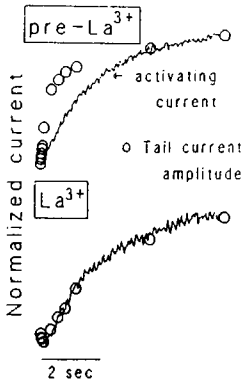

Th-AM-D6 CA^{2+} ACTIVATED INWARD CURRENTS IN SINGLE RABBIT VENTRICULAR CELLS. Y. Shimoni and W. Giles, Dept. of Medical Physiology, University of Calgary.

In rabbit ventricular cells, depolarizing voltage clamp pulses activate an inward 'tail' current. At -40 mV in normal Tyrode's solution, this current, which probably reflects the activity of the Na^+/Ca^{2+} exchanger, has a peak magnitude of 25-60 pA (immediately after a 100 msec depolarization to 0 mV), and decays back to the holding current level within 400-700 msec. We have further characterized this current, labelled I_{ex}. It is increased by increasing the intracellular sarcoplasmic reticulum calcium load. Thus, I_{ex} is larger after a rest period (30-60 sec), or following calcium loading obtained by inhibition of the Na^+-K^+ pump. We have also compared I_{ex} to the transient inward (TI) current, which is also elicited under calcium-loaded conditions. These two currents appear to be modulated by the same intracellular calcium transient, since I_{ex} is markedly reduced when elicited during or closely following a TI. Nevertheless, we were able to dissociate or separate these currents by a variety of methods: 1) Repolarizing to negative (e.g. -90 mV) membrane potentials increased I_{ex} and abolished the TI current. 2) Ba^{2+} and Sr^{2+} abolished the TI with small (with Ba^{2+}) or no (with Sr^{2+}) change in I_{ex}. 3) Ryanodine (2 μM) abolishes the TI while I_{ex} is unaltered. 4) Lowering $[Na^+]_o$ reduces I_{ex} but induces TI's. Thus, although the I_{ex} and TI currents are both activated by transient increases in $[Ca^{2+}]_i$ the underlying mechanisms appear to be different. Supported by the Canadian MRC and Heart Foundation.

Th-AM-D7 Cl/HCO_3 EXCHANGE AND pH_i REGULATION IN CULTURED CHICK HEART CELLS.
S. Liu, D.R. Piwnica-Worms and M. Lieberman, Dept. Physiology, Duke Univ. Med. Ctr., Durham, NC.

To investigate the possible role of Cl/HCO_3 exchange in intracellular pH (pH_i) regulation in cultured heart cells (polystrands), we measured changes in ^{36}Cl efflux, Cl content, intracellular Cl activity (a^i_{Cl}) and pH_i. Cells equilibrated with ^{36}Cl in a HCO_3/CO_2-buffered salt solution and then exposed to SITS (0.1 mM), an anion exchange inhibitor, responded with an ~20% reduction in ^{36}Cl efflux rate constant. Removal of HCO_3/CO_2 (+HEPES) caused an increase in a^i_{Cl} and Cl content. Removal of Cl_o increased pH_i by 0.07 (n=2) in 10 min. Steady-state pH_i was 7.16±0.01 (n=25) in control solution and 7.23±0.01 (n=11) in HCO_3/CO_2-free solution. Removal of HCO_3/CO_2 (+HEPES) resulted in a rapid transient increase in pH_i (alkalinization) of 0.38±0.03 (n=15) that slowly regulated downward by 0.20±0.02 (n=15) in 5 min. Readdition of HCO_3/CO_2 caused a rapid transient decrease in pH_i (acidification) of 0.22±0.02 (n=15) that regulated upward by 0.15±0.02 (n=13) in 5 min. Removal of HCO_3 also increased a^i_{Cl}, which decreased on restoring HCO_3. The regulatory changes in pH_i and a^i_{Cl} were both sensitive to 0.1 mM SITS. Exposure to 10 mM NH_4Cl for 5 min (prepulse) transiently increased pH_i and a^i_{Cl}; removal of NH_4Cl caused a transient decrease in pH_i and a^i_{Cl} followed by a recovery of both to control values. Similar results were obtained for changes in Cl content (DIDS-sensitive) in response to an NH_4-prepulse (20 mM, for 15 min). The rate of pH_i recovery was decreased by 25-45% in the presence of 1 mM amiloride and was completely blocked by the addition of 1 mM DIDS. Removal of Cl_o (± amiloride) following an NH_4-prepulse (10 mM, for 5 min) accelerated the pH_i recovery. These results suggest that Cl/HCO_3 exchange can regulate pH_i in response to intracellular acidification and alkalinization. Supported by HL27105, HL17670, HL07101.

Th-AM-D8 ACETYLCHOLINE-SENSITIVE K^+ CHANNELS IN HUMAN ATRIAL MYOCYTES.
R Sato, I Hisatome, RT Wiedmann, CE Arentzen, JA Wasserstrom, DH Singer, Northwestern Univ., Chicago, IL.

Acetylcholine (Ach)-K^+ channel activity was recorded from isolated human right atrial appendage myocytes using patch clamp techniques. The pipette solution contained 145 mM KCl and 5 mM HEPES at pH 7.4. Recordings from cell attached or from inside-out patches were obtained during exposure to Tyrode's solution containing 5.4 mM K^+ or an internal solution containing 145 mM K^+, respectively. Channel activity occurred in bursts and exhibited current-voltage relationships similar to those reported for other species. Ach-K^+ channels in cell attached patches had a mean open time of 2.5 ± 0.2 ms (n=4) when 10 μM Ach was present in the pipette. Mean closed time was 4.2 ± 0.2 ms (n=4). Slope conductance of inward current was 50 ± 3 pS (n=4). When the Ach concentration was increased from 1 μM to 10 μM, mean closed time decreased from 8.5 ± 0.4 ms to 4.2 ± 0.2 ms (n=4) without changes in mean open time. When the patch was detached from the membrane (inside-out patch), Ach-K^+ channel activity decreased. Upon addition of GTP or GTPγS to the bath, channel openings resumed. The current-voltage relation was nearly the same as for the cell attached patch. The presence of Ach was not required in the pipette in the GTPγS experiments. We conclude that: 1) overall, Ach-K^+ channels in human atrial myocytes are similar to those in other species; 2) however, the rate of reduction of channel closed time is less sensitive to Ach than in other species; 3) intracellular GTP (with Ach) or GTPγS (without Ach) activates this channel. The reduced Ach sensitivity may reflect a species difference. Alternately, differences in Ach sensitivity could be due to disease, in which case they could contribute to reduced diastolic potential levels reported in human atrium.

Th-AM-D9 A NEW TECHNIQUE FOR MEASURING THE LONGITUDINAL RESISTANCE IN STRANDS OF CARDIAC MUSCLE.
Bradley J. Roth and John P. Wikswo, Jr., Living State Physics Group, Dept. of Physics and Astronomy, Vanderbilt University, Nashville, TN 37235.

We have developed a new technique to determine the longitudinal resistance of a strand of cardiac muscle by simultaneously measuring the transmembrane action potential and the longitudinal action current. We threaded a guinea pig papillary muscle through a wire-wound, ferrite-core toroid that acts like a transformer, with the induced current in the winding proportional to the action current threading the toroid. The transmembrane potential was measured using a glass microelectrode. To interpret the data, we developed a mathematical model relating the potential and current produced by a strand of cardiac tissue surrounded by a toroid and lying in a saline bath. The electrical properties of the tissue are represented as a bidomain, which takes into account the anisotropy of the tissue and the presence of the interstitial space. With this model we can calculate the current through the toroid from the measured transmembrane potential. By fitting this calculated current to our measured current, we determined that the intracellular longitudinal conductivity, a lumped parameter with contributions from both the conductivity of the myoplasm and the conductance of the gap junctions, is 0.15±0.07 S/m. We observed no change in this value, to within the experimental error, when the extracellular potassium ion concentration was changed from 4 to 12 mM. (Supported by the Office of Naval Research under contract N00014-82-K-0107 and by National Institutes of Health grant 1-R01 NS 19794-01).

Th-AM-D10 EFFECTS OF CLASS 1 ANTIARRHYTHMIC AGENTS ON THE Ca CURRENT IN SINGLE VENTRICULAR CELLS OF THE FROG HEART. F. SCAMPS, A. UNDROVINAS & G. VASSORT, Physiologie Cellulaire Cardiaque, INSERM U-241, Université Paris-Sud, bât. 443, 91405 Orsay France.

The experiments were performed on single ventricular frog heart cells with the whole-cell patch clamp technique. The Ca current (I_{Ca}) was elicited by a 200 ms depolarization to 0 mV from a holding potential (HP) at -80 mV at 0.125 Hz . Na and K currents were blocked by TTX and Cs. Quinidine induced a reversible rest block of I_{Ca} with an ED_{50} at 10 µM. It also slowed down reactivation. This last effect was amplified at less negative HP and with increasing drug concentrations. The f and I-V curves were shifted 5 mV towards hyperpolarisation by Quinidine indicating that there was no voltage dependent inhibition. Flecainide induced similar alteration in I_{Ca} with an ED_{50} at 30 µM, except that there was no shift in f and I-V curves. Both drugs induced no frequency-dependent block of I_{Ca}. A phenotiazine, Ethmozin had a weak rest block (≈ 10%) even at high dose (25 µM). However, increasing the stimulation rate to 1.0, 1.6, 2.0 and 2.5 Hz reduced I_{Ca} to 75%, 69%, 46% and 30% of control respectively. A derivative, Ethacyzin induced both rest and frequency-dependent blocks. None of the drugs induced significant changes in I_{Ca} time to peak and inactivation rate. Thus, Quinidine and Flecainide might have a profound antiarrhythmic activity by inhibiting I_{Ca} and slowing its recovery. Ethmozin and Ethacyzin because of use-dependent block would be more efficient on post-depolarization. The above data indicate that, in cardiac cells, antiarrhythmic efficiency of class I antiarrhythmic agents might be due not only to I_{Na} but also to I_{Ca} inhibition.

Th-AM-D11 HYPERPOLARIZATION - ACTIVATED CURRENT IN EMBRYONIC CHICK VENTRICULAR MYOCYTES RESEMBLES I_{k1}. J. Satin and R. L. DeHaan, Anatomy and Cell Biol., Emory Univ. Health Sciences Center, Atlanta, GA 30322

Hyperpolarizing voltage steps elicit an inactivating I_{k1}-like current from isolated 7-day ventricle cells. Cells were patch-clamped in the whole cell recording mode at 22°C. Pipettes contained (in mM): KCl 125, KH_2PO_4 1, $MgCl_2.6H_2O$ 4, EGTA .1, Hepes 10, Na_2-ATP 3, Na-Phosphocreatine 3, pH 7.1, and the superfusate consisted of (in mM): KCl 2.5, NaCl 142, $CaCl_2.2H_2O$ 1.8, Hepes 10, pH 7.4. Voltage steps to -120 mV from a holding potential of 0 mV activated an inward current whose inactivation was best fit with a double exponential with typical time constants of 75 msec and 4.5 seconds. The mean peak amplitude was 23.8 ± 13.8pA (n=6). Increasing $[K^+_{out}]$ from 2.5 to 5.5 to 11.3 mM slowed the mean time to peak from 8.1 to 10.8 to 13.8 ms, respectively (n=5), and shifted the reversal potential from about -95 to -70 to -55 mV consistent with the change in E_k. The current displayed inactivation and inward rectification negative to E_k, thus resembling the Ba^{2+}-sensitive I_{k1} reported by DiFrancesco et al. (Pflug. Archiv. 402: 446-453, 1984). The inward rectification and reversal near E_k suggest that the current in 7-day ventricle cells is primarily K^+-selective, but the presence of inward current at $V_{com}=E_k$ indicates a small Na^+ permeability. Preliminary data from 4-day cells reveal a similar time-dependent current with a larger amplitude in 2.5 mM K^+_{out}. Further investigation will determine whether the developmental change in I_{k1} amplitude is due to changes in K^+ selectivity between 4-day and 7-day cells. (Supported by NIH grant HL-27385 to RLD)

Th-AM-D12 INACTIVATION OF I_{K1} INDUCED BY MONOVALENT CATIONS. **R.D. Harvey and R.E. Ten Eick Department of Pharmacology, Northwestern University, Chicago, IL 60611**

Inward-rectifying K^+ current (I_{K1}) was studied in isolated cat ventricular myocytes using a whole cell patch clamp technique. I_{K1} was elicited by 75 ms voltage clamp steps to membrane potentials more negative than E_K from a holding potential of -40 mV. Under control conditions ($[Na^+]_o$ = 140 mM) current evoked at potentials more negative than -145 mV exhibited a time-dependent decline resulting in a negative slope region in the steady-state (SS) current-voltage (I-V) relationship. The mechanism responsible for the current decline was investigated. A time-dependent shift of E_K following a conditioning pulse to -170 mV (-7.1 ±1.4 mV after 75 ms) suggested that depletion of extracellular K^+ was only partially responsible for the decline. The voltage dependence of SS inactivation indicated that depletion could not account for the negative slope region in the SS I-V relationship. Removal of extracellular Na^+ eliminated the negative slope region suggesting that the inactivation process responsible for this phenomenon was due to a voltage dependent block of I_{K1} by the monovalent cation. In the absence of Na^+ inactivation could be induced by extracellular Li^+ or Cs^+. Calculation of the electrical distance for binding of these ions yielded δ values of 1.57 (Na^+), 1.18 (Li^+), and 1.34 (Cs^+). Estimation of K_d values suggested the potency of inactivation sequence was $Cs^+ >> Na^+ > Li^+$. The findings suggest that inactivation of I_{K1} resulting in the negative slope region of the SS I-V relationship is caused by a time- and voltage-dependent block by Na^+ acting at a weak field strength binding site.

Th-AM-E1 SELECTIVITY OF A CATION-BINDING MEMBRANE SITE ESSENTIAL FOR EC COUPLING IN SKELETAL MUSCLE. G. Pizarro, R. Fitts and E. Rios. Department of Physiology, Rush Medical School, Chicago and Marquette University, Milwaukee.

Brum *et al.* (Biophys. J. 51: 552a) showed that Ca release from the sarcoplasmic reticulum and intramembrane charge movement in skeletal muscle require the presence of extracellular metal ions; in their complete absence the fibers have no contractility, no Ca release and a distribution of mobile charge characteristic of inactivated states. They interpreted these results as due to the existence of an "essential" cation binding site on the membrane-resident voltage sensor of EC coupling: the sensor inactivates when the site is not occupied. We now report that all ions in groups IA and IIA of the periodic table support EC coupling to some extent. We recorded Ca transients in voltage-clamped frog cut twitch fibers loaded with a Ca-sensitive dye, in solutions containing 100 mM of an ion in group IA as the sole metal ion; the Ca transients (and the release fluxes derived from the transients) had different magnitudes in the presence of different ions; the order of magnitudes was **Li>Na>K>Rb>Cs**. Release in 2 mM Ca was greater than in 100 mM Li. In the presence of 2 mM of alkali-earths the sequence was **Ca>Sr>Mg>Ba**. This is very similar to the sequence of ionic affinities of an intrapore binding site in the cardiac L-type Ca channel (as derived from permeability data of Hess et al., J. Gen. Physiol. 88: 293). If the magnitude of Ca release in the presence of a cation was determined by its affinity for the essential site, the profile of affinities of this site would be very similar to that of the Ca channel site. This suggests that the sensor molecule contains a region analogous to the Ca channel pore. Other evidence of similarity is presented in this meeting (Fill *et al.*). Supported by NIH.

Th-AM-E2 COMPLETE SEPARATION OF CHARGES 1 AND 2 IN FROG SKELETAL MUSCLE FIBERS. E. Rios, M. Rodriguez, G. Pizarro, R. Fitts and G. Brum. Department of Physiology, Rush Medical School, Chicago, Marquette University, Milwaukee and University of Montevideo, Uruguay.

Twitch fibers kept at a depolarized holding potential (HP = 0 mV) have an intramembrane mobile charge named Charge 2 that characteristically moves at large negative voltages. Upon changing HP to a normally polarized HP (-100 mV) Charge 2 is reduced but not eliminated, and Charge 1 appears. It has been suggested that Charge 2 corresponds to inactivated states of the voltage sensor of EC coupling, and converts to Charge 1 as the inactivated sensors "reprime" at -100 mV.

Extracellular Ca^{2+} is known to oppose the inactivation process; we now report that Charge 2 can be eliminated in the presence of high extracellular [Ca^{2+}]. In a 100 mM Ca^{2+} external medium, cut fibers held at HP = +40 mV had Charge 2 of normal magnitude and a transition voltage $\bar{V}$ = -73 mV. **At HP = -100 mV no charge moved in the voltage range of Charge 2**; all mobile charge in this condition appeared to be Charge 1, but large ionic currents prevented its measurement at positive voltages. In 215 mM $CoSO_4$ charge movements had similar properties as in 100 mM $Ca^{2+}$and there were no time-dependent ionic currents. This is then an "ideal" solution for the separate measurement of charges 1 and 2. **Charge 1** (measured at HP = -100 mV) had Boltzmann parameters: Q_{max} = 40nC/μF, $\bar{V}$ = -8 mV, K = 18 mV; **Charge 2** (measured at HP = 40 mV) had Q_{max} = 34 nC/μF, $\bar{V}$ = -80 mV, K = 23mV. The apparent density of charged particles, derived from these parameters, is about the same for charges 1 and 2 and greater than earlier estimates. The disappearance of Charge 2 in normally polarized fibers in high Ca^{2+} (or Co^{2+}) will be interpreted as a conversion of Charge 2 to Charge 1, in a reaction promoted by binding of Ca^{2+} (Co^{2+}) to the voltage sensor of EC coupling.

Th-AM-E3 PHENYLGLYOXAL BLOCKS CHARGE MOVEMENT AND E-C COUPLING IN FROG SKELETAL MUSCLE. Elaine F. Etter, Dept. of Biol. Chem., Univ. of Maryland Sch. of Med., Baltimore, MD 21201.

The arginine-specific protein-modifying reagent, phenylglyoxal (PGO), was reported to block contraction in intact frog skeletal muscle fibers without affecting resting membrane potential, action potentials, or caffeine contractures (Fujino, M., Proc. Intl. Union Physiol. Sci., XVI:P313.19, 1986). The effects of PGO on contraction threshold and charge movement were studied in cut single muscle fibers voltage clamped in a double Vaseline gap chamber (holding potential = -100mV). PGO shifted the strength-duration curve for pulses required to produce just-detectable contractions toward more positive voltages and longer durations. Charge movement transients were recorded in other fibers with contraction blocked by internal EGTA (5mM in the end pool solution). The reaction with arginine is facilitated by alkaline pH, therefore PGO was applied, externally, at pH=8.0 (T=12°C). Charge movement was recorded under these same conditions. Charge vs. voltage relations, expressed as $Q=Q_{max}/(1+\exp(-(V-\bar{V})/k))$, were determined from measurements before and after PGO treatment. A 10 min treatment with 11mM PGO decreased Qmax by 20% and increased k from 15 ±2mV to 20 ±2mV (n=3), without shifting $\bar{V}$. When large pulses were used (to 0 to 30 mV) to monitor changes in Qmax, treatment with 14mM PGO for 18-25 min decreased Qmax by 45% ±5% (n=4). Qmax decreased with a time constant of 6 min. After PGO was washed away, Qmax partially recovered with a time constant of 15 min. The linear capacitance, measured by -20mV steps every 2-5 min before, during and after long treatments, remained constant within 5% (8 fibers), even when Qmax was maximally decreased. Thanks to Dr. Fujino for communicating unpublished results.

Th-AM-E4 EFFECTS OF BDM ON CONTRACTILE AND MEMBRANE ELECTRICAL PROPERTIES IN FROG TWITCH FIBERS. Chiu Shuen Hui, Dept. of Physiol. and Biophys., Indiana University Medical Center, Indianapolis, IN 46223 and James Maylie, OB Research, Oregon Health Science University, Portland, OR 97201.

2,3-butanedione monoxime (BDM) was reported to block contraction in skeletal muscle by selectively interfering with cross-bridge formation (Mulieri and Alpert, Biophys. J. **45**, 47a, 1984). We extended their work to cover a wider range of BDM concentration, from 0.25 to 20 mM. Single intact fibers were isolated from semitendinosus muscles of *Rana temporaria* and stimulated extracellularly. Twitch tension was recorded at 5-6°C. In most of the fibers, 10 mM BDM was not sufficient to block contraction completely. The dose-response curves for fibers stretched to sarcomere spacing of 3.0 μm and 3.6 μm were not noticeably different. The half-blocking concentration of BDM is 0.43 mM, averaged over 10 fibers. We also studied the effect of BDM on action potential in bundles of fibers at 5°C. We found that 5 and 10 mM BDM did not affect the peak amplitude but prolonged the half-width by 1.5 and 3 times, respectively, whereas 20 mM BDM reduced the peak amplitude by about 1/5 and prolonged the half-width more than 10-fold. Furthermore, we studied the effect of 20 mM BDM on charge movement which was measured at the end of a fiber in a halved semitendinosus muscle using the 3-microelectrode voltage clamp technique at 3-6°C. Both components of charge, Q_β and Q_γ, look very normal. The best fit parameters for the steady-state voltage distribution are: Q_{γ}^{max} = 18.3 nC/μF, k = 8.4 mV and V′ = -27.2 mV (N = 8), which fall within the ranges of those measured in control situation. It thus appears that, under voltage clamp condition, BDM does not affect charge movement, which is believed to play the role of voltage sensor in E-C coupling. (Supported by NS 21955 and AM 35737)

Th-AM-E5 EFFECTS OF BDM ON ANTIPYRYLAZO III CALCIUM SIGNALS IN FROG CUT TWITCH FIBERS. James Maylie, OB Research, Oregon Health Science University, Portland, OR 97201 and Chiu Shuen Hui, Dept. of Physiol. and Biophys., Indiana University Medical Center, Indianapolis, IN 46223

We have shown that BDM suppresses contractility without affecting charge movement. Calcium signals were measured in cut twitch fibers at 16°C (Irving, Maylie, Sizto and Chandler, 1987) to see whether BDM affects calcium release. Changes in light intensity at 810 nm, a wavelength not absorbed by Antipyrylazo III, was used to monitor the intrinsic optical properties of the fibers. BDM reduced the 810 nm intrinsic signal in action potential stimulated fibers in a concentration-dependent manner. In 2 mM BDM, the reduction was about 50%. Calcium transients following an action potential were also reduced by BDM but to a lesser degree. On the average, the peak of the calcium transient was reduced to 79%, 76% and 49% in 5, 10 and 20 mM BDM, respectively. The effects of BDM on the calcium transient were associated with an elevation of the afterpotential from about -75 mV in normal Ringer to -70, -63 and -52 mV in 5, 10, and 20 mM BDM, respectively. In voltage clamp mode, the calcium transients elicited by a 5 ms pulse to 0 mV, used to mimic an action potential, were reduced to 53% and 49% in 10 and 20 mM BDM, respectively. 10 mM BDM generally shifted the voltage threshold for the first detectable calcium transient 3 to 5 mV to more negative potentials. The voltage dependence of the calcium transient near threshold was also reduced by 10 mM BDM with the e-fold factor increased from 2.4 mV in control to 3.4 mV in 10 mM BDM. The effects of BDM described are completely reversible. The results show that BDM affects both movement related optical signals and the release of calcium but with different concentration dependence. (Supported by AM 35737 and NS 21955)

Th-AM-E6 CURRENTS ASSOCIATED WITH INTRAMEMBRANOUS CHARGE MOVEMENT IN FROG CUT TWITCH FIBERS. Chiu Shuen Hui and W. Knox Chandler. Department of Physiology and Biophysics, Indiana Medical School, Indianapolis, IN and Department of Physiology, Yale Medical School, New Haven, CT.

Semitendinosus fibers from R. temporaria were mounted in a double Vaseline-gap chamber with a TEA-Cl solution in the central pool, at 13-14°C, and a Cs-glutamate solution containing 20 mM-EGTA in the end pools. Following a voltage step from -90 mV to near threshold (-60 to -50 mV), the outward charge movement current has an early component, Q_β, and a more slowly developing component, Q_γ, that lasts 100-400 ms. If the threshold step is preceded by a prepulse to -40 mV, the inward charge movement current also has two components, one that decays within 10-30 ms, Q_β, and another that decays within 100-300 ms, Q_γ. If the threshold pulse is brief and the fiber is repolarized to -90 mV before the Q_γ current has completely decayed, but after the Q_β current has done so, the (inward) current at -90 mV contains a contribution from Q_γ that moved during the -40 mV prepulse. This method has been used to estimate Q_γ at -40 mV and at other voltages. In a typical experiment, the resulting Q_γ vs. V curve was fitted by a Boltzmann equation with $V_{1/2}$ = -63 mV and k = 3.8 mV. The Q vs. V curve for total charge was also fitted by a Boltzmann curve, with $V_{1/2}$ = -55 mV and k = 7.6 mV, but was better fitted by the sum of two Boltzmann curves of approximately equal amplitude. One curve, tentatively identified with Q_β, has $V_{1/2}$ = -44 mV, k = 14 mV and another, identified with Q_γ, has $V_{1/2}$ = -58 mV, k = 3.6 mV. These experiments show that charge movement currents in cut fibers, similar to those in intact fibers, can be resolved into Q_β and Q_γ components and that the position and steepness of the Q_γ vs. V curve are similar to those of the peak [Ca] vs. V curve obtained under similar conditions (Maylie, Irving, Sizto, and Chandler, 1987, JGP, 89: 83). Supported by NS-21955 and AM-37643.

Th-AM-E7 CALCIUM TRANSIENTS IN FROG CUT TWITCH FIBERS MEASURED WITH 1,1'-DIMETHYLMUREXIDE-3,3'-DIACETIC ACID. Akihiko Hirota, W. Knox Chandler, Philip S. Southwick, and Alan S. Waggoner. Department of Physiology, Yale University School of Medicine, New Haven, CT and the Departments of Chemistry and Biological Sciences, Carnegie Mellon University, Pittsburgh, PA.

Following action potential stimulation of a cut semitendinosus fiber from R. temporaria, there is a transient increase in myoplasmic free [Ca]. At 18°C, the peak value measured with tetramethylmurexide (TMX) is approximately 20 μM (Maylie, Irving, Sizto, Boyarsky, and Chandler, 1987, JGP, 89: 145). Two observations, however, suggest that TMX is not confined to the myoplasmic space but may enter the sarcoplasmic reticulum (SR). First, the resting absorbance spectrum indicates that 10^{-4} 10-15% of the indicator is complexed with Ca, although resting myoplasmic free [Ca] is less than 10^{-4} times the indicator's K_D (=2.6 mM). Second, the Ca-related change in TMX absorbance shows an early peak followed by a maintained component of opposite sign, suggesting dissociation of some of the resting Ca-TMX complexes (perhaps as a consequence of Ca release from the SR). To limit the access of indicator to the SR space, we synthesized a less permeant analogue of TMX (K_D=0.8 mM) in which two of the methyl groups were replaced with acetate groups. In a resting cut fiber, the absorbance spectrum of the new indicator matches that of Ca-free indicator in a cuvette. Following action potential stimulation, the change in indicator absorbance has a wavelength dependence that matches the cuvette Ca-difference spectrum, an amplitude that varies linearly with indicator concentration (as does TMX) and corresponds to peak free [Ca] = 15-40 μM, and little or no maintained component. A disadvantage of this indicator, as well as others (Maylie et al., 1987, JGP, 89: 41-176), is that not all of it is freely dissolved inside myoplasm; 22-34% appears to be bound to intracellular constituents and consequently may not react normally with Ca. Supported by AM-37643.

Th-AM-E8 EFFECT OF INTRACELLULAR RUTHENIUM RED ON EXCITATION-CONTRACTION COUPLING IN SKELETAL MUSCLE. S. M. Baylor, S. Hollingworth and M. W. Marshall. Departments of Physiology, Univ. of Pennsylvania, Philadelphia, PA and University of Newcastle, Newcastle-upon-Tyne, England.

The ability of Ruthenium Red (RR) to block sarcoplasmic reticulum (SR) Ca^{2+} permeability in fractionated preparations has been used in recent biochemical studies as a marker for the physiological Ca^{2+} release pathway. However, the ability of intracellular RR to block SR Ca^{2+} release in living muscle fibers has not previously been demonstrated. In order to investigate this question, intact single twitch fibers from frog were micro-injected with RR (Sigma Chemical Co.). Myoplasmic RR concentration, determined by absorbance measured at 540 nm, varied along the fiber axis between 0 and 200 μM. The "second" component of the intrinsic birefringence signal (Baylor and Oetliker, 1975), the amplitude and time course of which are closely correlated with the myoplasmic free Ca^{2+} transient, was used to assess RR's effect on excitation-contraction coupling. RR was found to block the birefringence signal in a dose-dependent manner, without alterations in the action potential. From RR's apparent diffusion constant in myoplasm, $0.03 \times 10^{-6} cm^2 s^{-1}$ (16 °C), the bound/free ratio of RR was estimated to be about 30:1. From this, the free concentration of RR which reduced the birefringence signal by 50% was estimated to be 1-2 μM. The similarity in concentration dependence of RR's block in intact and disrupted preparations suggests that a common blocking site is involved.

In order to learn more about the mechanism of the block, the effect of RR on membrane charge movements (Schneider and Chandler, 1973) was studied using the 3-micro-electrode, middle-of-the fiber voltage clamp (Adrian and Marshall, 1977). At concentrations similar to those which effectively suppressed the birefringence signal, RR injected into frog fibers had no discernible effect on sub-threshold charge measured in isotonic solution at 2-6 °C.

Th-AM-E9 CALCIUM TRANSIENTS IN VOLTAGE CLAMPED GIANT BARNACLE MUSCLE FIBERS.

J. Vergara* and P. Verdugo+, *Department of Physiology, UCLA, Los Angeles, CA 90024, +Center for Bioengineering, U. of Washington, WA 98195, and Friday Harbor Laboratories, WA 98250.

Giant barnacle muscle fibers from Balanus nubilus are characterized by the presence of a voltage dependent regenerative Ca conductance which is responsible for their excitable characteristics and for the entry of Ca ions required to trigger the contractile machinery. In order to investigate whether contraction relies only on this Ca entry from the extracellular medium or if there is a significant contribution from intracellular release by the sarcoplasmic reticulum (SR), optical experiments were performed on fibers voltage clamped and perfused internally with the Ca indicator azol. In addition, some fibers were stained with the potentiometric dye NK2495 to detect membrane potential changes within the clefts and tubules abundant in this preparation. The results can be summarized as follows: a) The inward flow of Ca ions is an absolute requisite for the detection of Ca transients in this muscle preparation. Removal of external Ca, or large depolarizations to values close to the reversal potential for this ion, result in the absence of signals. Ba replaces Ca only in that it generates currents larger than the Ca currents, but it does not elicit Ca transients. b) The time course of the intracellular Ca transients is faster than the integral of the Ca current, qualitatively suggesting a contribution from intracellular stores. The addition of neomycin to the intracellular perfusate results in a reduction of fast components in the Ca transients and a closer matching between both time courses. c) A quantitative comparison between the Ca entry from the extracellular bathing solution (sea water) and the value calculated from the Ca absorbance signals also suggests that an intracellular source contributes towards the change in intracellular Ca concentration. d) The presence of Ca and K conductances in clefts and tubules result in radial inhomogeneities of membrane potential which may account for the oscillatory behavior of the currents. In summary, our results are compatible with the possibility that, in barnacle muscle fibers, the entry of Ca ions triggers the release of Ca from the SR, the latter providing a moderate amplification mechanism to ensure a rapid homogeneous change in intracellular Ca concentration. Thanks to R.Y.Tsien for the gift of azol. Supported by MDA and NIH (AM25201).

Th-AM-E10 INTRACELLULAR Ca^{2+}-TRANSIENTS MEASURED WITH FURA-2 IN VOLTAGE-CLAMPED RAT AND FROG VENTRICULAR MYOCYTES. G. Callewaert, L. Cleemann and M. Morad. Department of Physiology, University of Pennsylvania, Philadelphia, PA 19104.

The voltage dependence of $[Ca^{2+}]_i$-transients were measured in whole cell clamped rat and frog ventricular myocytes loaded with fura-2. A mirror oscillating at 1.2 kHz was used as a mechanical light chopper for dual wave-length excitation at 330 and 410 nm. This system guarded against motion artifacts and gave, without signal averaging, a high signal to noise ratio. 200 ms duration voltage-clamp pulses were applied from a holding potential of -50 mV at a frequency of 0.1 Hz and the accompaning Fura-2 signals and membrane current were sampled on computer. In both rat and frog ventricular cells, the voltage dependence of the $[Ca^{2+}]_i$-transients was bell-shaped and was similar to the voltage dependence of i_{Ca} (shown for rat in figure). The amplitudes of the $[Ca^{2+}]_i$ transients and of i_{Ca} were enhanced by 1 uM epinephrine in both preparations. The rate of decline of the $[Ca^{2+}]_i$-transients was also enhanced by epinephrine in the rat, such that at potentials positive to +70 mV a net decrease of $[Ca^{2+}]_i$ occurred. The $[Ca^{2+}]_i$-transient in the frog heart was related to the integral of i_{Ca}. In the rat cells the $[Ca^{2+}]_i$-transients were strongly suppressed by ryanodine. These results suggest that the $[Ca^{2+}]_i$-transient in the frog is related to the influx of Ca^{2+} through the Ca^{2+} channel while in the rat it is related mainly to Ca^{2+} induced release of Ca^{2+} from the sarcoplasmic reticulum.

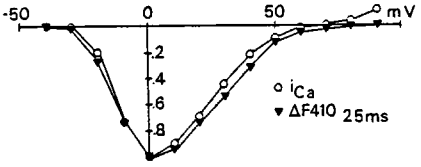

Th-AM-E11 THE LATE PHASE OF TWITCH RELAXATION IN UNLOADED SINGLE ADULT CARDIAC MYOCYTES IS ASSOCIATED WITH A DECREASE IN CYTOSOLIC Ca^{2+}. M. C. Capogrossi, H. A. Spurgeon, S. Raffaeli, M. D. Stern, and E. G. Lakatta (Intr. by Frank Yin). Laboratory of Cardiovascular Science, Gerontology Research Center, NIA, NIH, Baltimore, MD 21224

The late phase of twitch relaxation in unloaded adult single cardiac myocytes is slow. To determine whether this is related to a slow decrease in cytosolic Ca^{2+} (Ca_i), we used enzymatically dispersed left ventricular myocytes from 2-6 month old rats, loaded with 4 μM Indo-1 AM for 1.5-4 min. The 410/490 nm ratio of Indo-1 fluorescence following epi-illumination at 350+10 nm was taken as a measure of Ca_i. Cell length during field depolarization was simultaneously measured with a photodiode array (Hepes buffer; T 23°C, pH 7.4). Panel A: rested twitches in the same myocyte before (control in the Fig.) and after exposure to Indo-1 AM have an identical late phase of relaxation which after Indo-1 loading is paralleled by a slow decrease in Ca_i. Panel B: in the same cell twitches of similar amplitude obtained either by enhanced bathing $[Ca^{2+}]$ or isoproterenol show that only isoproterenol accelerates the decay of Ca_i and of the late phase of relaxation. In conclusion, the rate of removal of Ca_i appears to modulate not only the early but also the late phase of relaxation of the unloaded twitch.

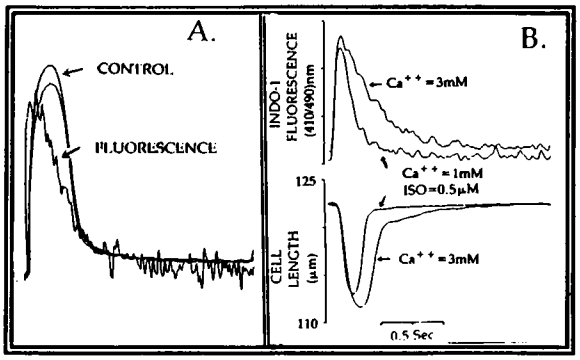

Th-AM-E12 **$[Ca^{2+}]_i$ MEASUREMENTS DERIVED FROM 5,5'-F_2-BAPTA (5FB) OR FURA-2 PROVIDE LOWER-LIMIT ESTIMATES OF GENUINE SPATIO-TEMPORAL AVERAGE $[Ca^{2+}]_i$** David T. Yue, Masafumi Kitakaze, and Eduardo Marban, Division of Cardiology, The Johns Hopkins Medical Institutions, Baltimore, MD

The nature of the errors introduced by spatio-temporal gradients of $[Ca^{2+}]_i$ seem complex for the newer generation of $[Ca^{2+}]_i$ indicators, owing to the processing of indicator signals involved in making an estimate of spatio-temporal average $[Ca^{2+}]_i$ ($\langle[Ca^{2+}]_i\rangle$). For 5FB, the estimate of $\langle[Ca^{2+}]_i\rangle$ ($\langle[Ca^{2+}]_i\rangle_{est}$) equals $K_d*\langle B\rangle/\langle F\rangle$, where $\langle B\rangle$ and $\langle F\rangle$ are the areas under the Ca- bound and free peaks of 5FB's spatio-temporally averaged ^{19}F NMR signals. Hence, understanding the effect of $[Ca^{2+}]_i$ gradients upon $\langle[Ca^{2+}]_i\rangle_{est}$ seems to require consideration of a complicated entity: the ratio of two spatio-temporally averaged signals. However, $\langle B\rangle$ and $\langle F\rangle$ are not independent of each other (constant=$\langle B\rangle+\langle F\rangle$), and consequently $\langle[Ca^{2+}]_i\rangle_{est}$ is uniquely determined by $\langle B\rangle$ or $\langle F\rangle$ alone. Consideration of the behavior of any one of these with respect to spatio-temporal gradients of $[Ca^{2+}]_i$ is sufficient to understand the others. Then, arguing from interdependence, and the fact that B plotted vs $[Ca^{2+}]_i$ is downwardly convex, just as for quin-2, we conclude that 5FB yields a lower-limit estimate of $\langle[Ca^{2+}]_i\rangle$. The figure illustrates this point by plotting the time-resolved $[Ca^{2+}]_i$ transient (squares and fitted curve) of a perfused ferret heart loaded with 5FB. True time-average $[Ca^{2+}]_i$ (dashed line, 540 nM), derived from the transient, exceeds the estimate of $[Ca^{2+}]_i$ obtained from temporally averaged NMR signals (flat solid line, 350 nM). Analogously for fura-2, $\langle F_{340}\rangle$, $\langle F_{380}\rangle$, and $\langle[Ca^{2+}]_i\rangle_{est}$ ($=K_d*(S_{f2}/S_{b2})*(\langle F_{340}\rangle/\langle F_{380}\rangle-R_{min})/(R_{max}-\langle F_{340}\rangle/\langle F_{380}\rangle)$) are interdependent, and F_{340} plotted vs $[Ca^{2+}]_i$ is downwardly convex. Thus, fura-2 will also underestimate true $\langle[Ca^{2+}]_i\rangle$. These results caution that, like the simpler indicator quin-2, 5FB and fura-2 can appreciably underestimate true $\langle[Ca^{2+}]_i\rangle$ in the setting of spatio-temporal gradients of $[Ca^{2+}]_i$.

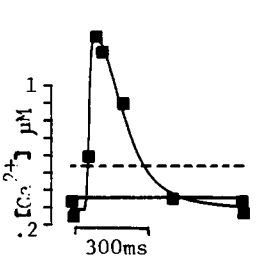

Th-AM-E13 CA^{2+} TRANSIENTS IN INTACT PERFUSED HEARTS OBSERVED BY ^{19}F NMR SPECTROSCOPY

M.M. Pike, M. Kitakaze, V.P. Chacko and E. Marban: Johns Hopkins Medical Institutions

Previous measurements of Ca^{2+} transients have been restricted to superfused muscle or dissociated cells. However, using ^{19}F NMR spectroscopy of fluorinated Ca indicators, detection of $[Ca^{2+}]_i$ in perfused hearts has recently become possible, but with limited time resolution (1,2). Here, we report that gated ^{19}F NMR provides time-resolved measurements of $[Ca^{2+}]_i$ in perfused hearts. Ferret hearts, perfused at 30°, with a modified HEPES Tyrode solution, and loaded with 5,5'-F2 BAPTA were placed in a Bruker AM-360 NMR spectrometer (8.46T). Hearts were paced at 0.9-1.6 Hz and developed pressure recorded. The NMR data acquisition was gated according to a programmable delay from the pacing stimulus. Families of ^{19}F (or ^{31}P) spectra corresponding to various times in the cardiac cycle were acquired. For 16 hearts in 8mM $[Ca^{2+}]_o$, the mean $[Ca^{2+}]_i$ increased from 202 ± ηM (mean ± SEM) at 10-20 msec before stimulation to 1660 ± ηM at 75-125 msec after stimulus. The figure shows data from one such heart. As expected, the $[Ca^{2+}]_i$ peaked much earlier than did the ventricular pressure. Gated ^{31}P spectra showed no apparent oscillations during the cardiac cycle. These results demonstrate the possible utility of this technique in elucidating the mechanisms which regulate contractility in the whole heart.

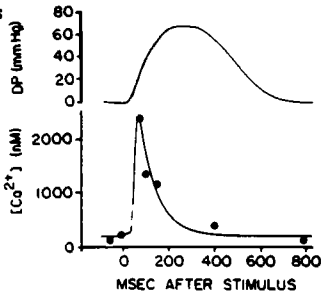

1. E. Marban et al., PNAS, 84, 6005 (1987)
2. C. Steenbergen et al., Circ. Res., 60, 700 (1987)